

pubs.acs.org/JPCB Review Article

Protein Phase Separation Arising from Intrinsic Disorder: First-Principles to Bespoke Applications

Daniel Mark Shapiro, Max Ney, Seyed Ali Eghtesadi, and Ashutosh Chilkoti*



Cite This: J. Phys. Chem. B 2021, 125, 6740–6759

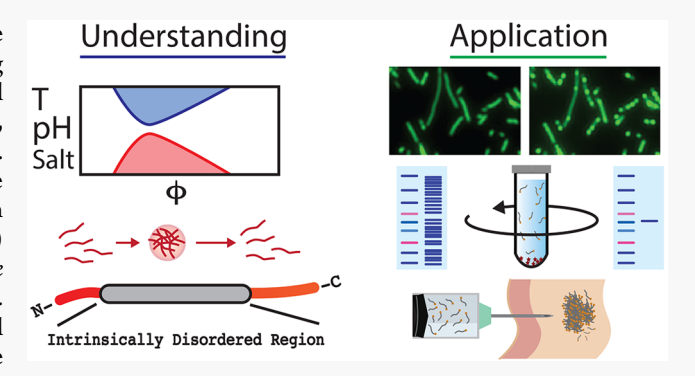


ACCESS

Metrics & More

Article Recommendations

ABSTRACT: The phase separation of biomolecules has become the focus of intense research in the past decade, with a growing body of research implicating this phenomenon in essentially all biological functions, including but not limited to homeostasis, stress responses, gene regulation, cell differentiation, and disease. Excellent reviews have been published previously on the underlying physical basis of liquid—liquid phase separation (LLPS) of biological molecules (*Nat. Phys.* 2015, 11, 899—904) and LLPS as it occurs natively in physiology and disease (*Science* 2017, 357, eaaf4382; *Biochemistry* 2018, 57, 2479—2487; *Chem. Rev.* 2014, 114, 6844—6879). Here, we review how the theoretical physical basis of LLPS has been used to better understand the behavior of biomolecules that undergo LLPS in natural systems



and how this understanding has also led to the development of novel synthetic systems that exhibit biomolecular phase separation, and technologies that exploit these phenomena. In part 1 of this Review, we explore the theory behind the phase separation of biomolecules and synthetic macromolecules and introduce a few notable phase-separating biomolecules. In part 2, we cover experimental and computational methods used to study phase-separating proteins and how these techniques have uncovered the mechanisms underlying phase separation in physiology and disease. Finally, in part 3, we cover the development and applications of engineered phase-separating polypeptides, ranging from control of their self-assembly to create defined supramolecular architectures to reprogramming biological processes using engineered IDPs that exhibit LLPS.

1. INTRODUCTION TO PHASE SEPARATION

Liquid-liquid phase separation (LLPS) is the phenomenon wherein a heterologous mixture of two or more molecular species—components—spontaneously separates into two or more homogeneous "phases", and where each phase is enriched in one of the molecular species. An illustrative example of such a phase transition is that of salad dressing—a single phase separating into an oily phase and an aqueous phase. The analogous LLPS behavior of interest here is that of a class of intrinsically disordered proteins and protein polymers that exhibit similar behavior in a biological milieu. The study of this phase separation behavior in biology is grounded in the wellestablished body of knowledge on the phase separation of synthetic polymers in solution. In part 1 of this Review, we describe the foundational polymer physics theory underlying polymer phase separation and some of its modern expansions in section 1.1, describe a few examples of synthetic polymers that phase-separate in section 1.2, and finally discuss a few examples of phase-separating proteins and the role that this phase separation plays in their function in section 1.3.

1.1. Thermodynamics of Phase Separation. The foundational theory behind LLPS in polymers was first introduced by Flory and Huggins^{1,2} and has become the

groundwork upon which the study of the phase separation of macromolecules has been built. Flory—Huggins theory describes how the LLPS of a polymer is driven by the balance between the entropy of mixing and the energetic interactions between the polymer and solvent. For polymers dissolved in a solvent, the entropy of mixing is always positive, 4 so whether or not the mixture will undergo phase separation is dictated solely by the energetic contributions. The entropic and enthalpic contributions of mixing are typically calculated per site on a lattice that models the polymer—solvent system. After calculating the entropic and enthalpic contributions per site, one can calculate the Helmholtz free energy of mixing per lattice site. From the free energy, one can determine the binodal phase boundary (Figure 1a), below which the system can phase-separate, and the spinodal phase boundary (Figure 1a) which

Received: February 8, 2021 Revised: May 30, 2021 Published: June 18, 2021





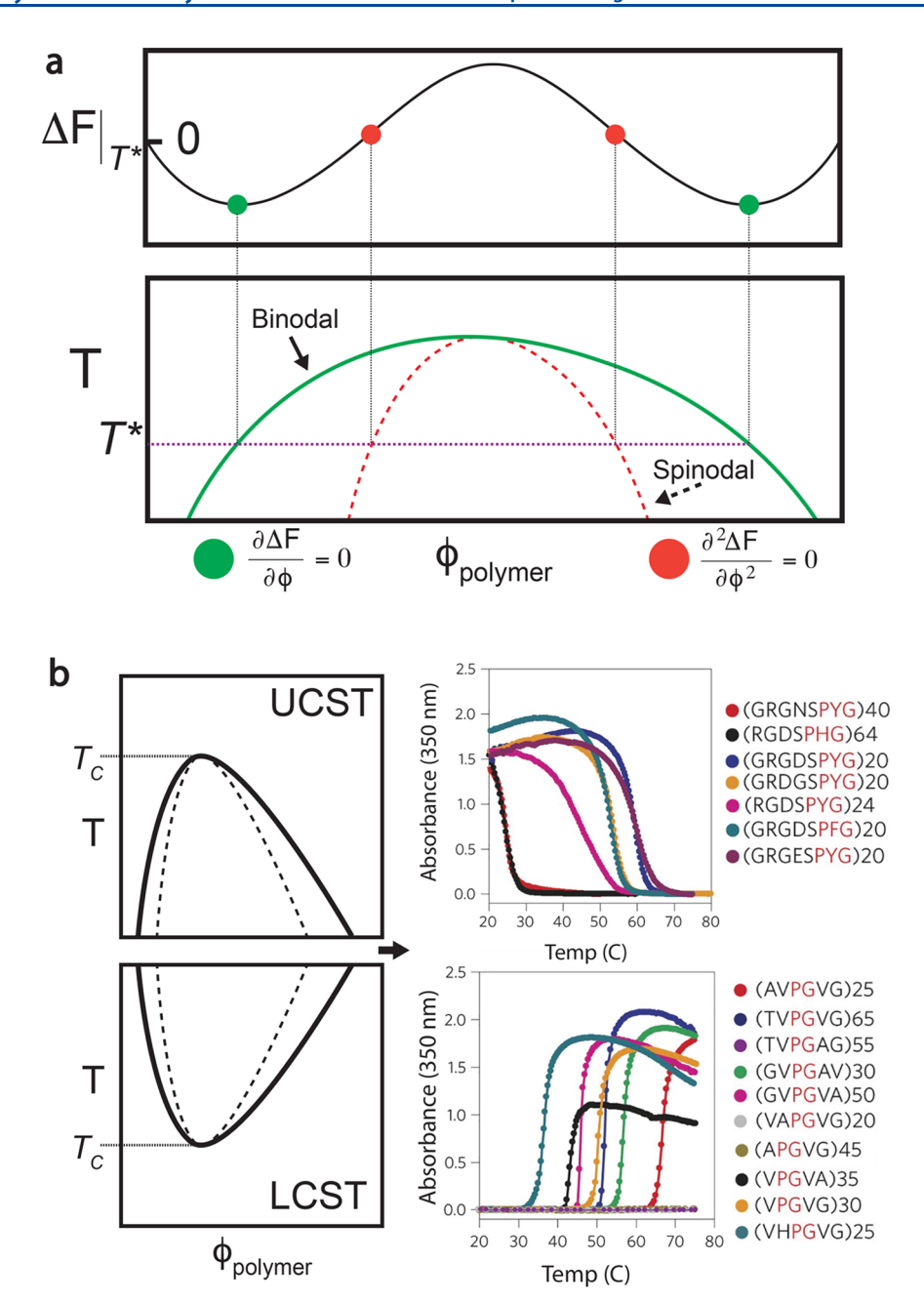


Figure 1. The phase diagram. (a) The phase diagram can be plotted by finding the free energy of the solution at a given T^* temperature and polymer concentration (ϕ) . The binodal boundary (green line) is constructed by finding the local minima (green dots represent local minima at a given T^*) of the free energy as a function of temperature, and the spinodal boundary (dotted red line) is constructed by finding the inflection points of the free energy (red dots represent inflection points at a given T^*) as a function of temperature. (b) UCST and LCST behavior of protein polymers can be determined by plotting the turbidity (absorbance at 350 nm) of the polymer as a function of temperature. For UCST polymers, the turbidity is high below the T_c as the polymers phase-separate out of solution but drops as the polymers dissolve. For LCST polymers, the turbidity is low below the T_c but sharply increases as the polymers phase-separate at the T_c . Turbidity data of synthetic protein polymers with sequences noted adapted from Chilkoti et al. with permission.

determines the stability of the phase-separated system and predicts how phase separation occurs, as a function of polymer concentration and environmental—solution—parameters such as temperature, pH, or salt. Within the spinodal phase boundary, the system will spontaneously phase-separate because of small fluctuations in composition, whereas, in the region between the spinodal and binodal boundaries, the system is metastable and will phase-separate upon the occurrence of sufficient nucleation events.

1.1.1. Flory—Huggins Theory to Describe Phase Separation in Polymer Solutions. The Flory—Huggins theory, utilizing a lattice model for calculations rooted in statistical mechanics, relies on a key assumption, namely, that the volume before and after mixing stays constant. This is not always true for the dissolution of polymers in a solvent, as the expulsion of solvent from the condensed phase changes the volume of lattice sites within the condensate. In practice, however, the Flory—Huggins theory models experimental data very well and has been

effectively used as a basis for describing the phase behavior in biological systems.⁵

Each lattice site volume is typically defined as the volume of the smallest molecular unit in the system, whether being a solvent molecule or roughly the excluded volume of one Kuhn monomer unit.⁶ Assuming the lattice has *n* sites, the entropy of mixing is

$$\Delta S_{\text{mix}} = n_{\text{s}} \Delta S_{\text{s}} + n_{\text{p}} \Delta S_{\text{p}}$$

where n is the number of occupied lattice sites, ΔS is the entropy, and the subscripts p and s refer to polymer and solvent, respectively. The number of sites occupied by the solvent molecules is equivalent to the volume fraction of the system that is solvent, ϕ_s , multiplied by the total number of sites n, $n_s = \phi_s n$, since each solvent molecule occupies one site by definition. The number of sites occupied by the polymer molecules is the volume fraction of the system that is polymer divided by the number of monomers in each polymer chain, ϕ_p/N_p , giving the volume fraction of the system that is polymer monomers,

multiplied by the total number of sites n, $n_{\rm p} = \frac{\phi_{\rm p}}{N_{\rm p}} n$. Flory—

Huggins theory assumes that each repeat unit in the polymer occupies one lattice site even if they are different in size from the solvent molecules.

Thus, for polymer solutions, the entropy of mixing per lattice site $\frac{\Delta S_{mix}}{a}$ is 4

$$\Delta S_{\text{mix/site}} = -k_{\text{B}} \left(\frac{\phi_{\text{p}}}{N_{\text{p}}} \phi_{\text{p}} + \phi_{\text{s}} \phi_{\text{s}} \right)$$

The energy of mixing per site can be expressed as a combination of interaction energies u_{i-i} within the polymer—solvent system:

$$\Delta U_{\text{mix/site}} = \frac{z}{2} \phi_{\text{p}} (1 - \phi_{\text{p}}) (2u_{\text{p-s}} - u_{\text{s-s}} - u_{\text{p-p}})$$

This is then expressed as

$$\Delta U_{\text{mix/site}} = \chi \phi_{\text{p}} (1 - \phi_{\text{p}}) k_{\text{B}} T$$

where the empirically determined interaction parameter χ describes the difference of interaction energies within the system where each site interacts with z neighboring sites:

$$\chi = \frac{z}{2k_{\rm B}T}(2u_{\rm p-s} - u_{\rm s-s} - u_{\rm p-p})$$

Together, the Helmholtz free energy of mixing per site for polymer solutions, also called the Flory—Huggins equation for polymer solutions, is expressed as

$$\Delta F_{\text{mix/site}} = \Delta U_{\text{mix/site}} - T \Delta S_{\text{mix/site}}$$

$$= k_{\text{B}} T \left[\frac{\phi_{\text{p}}}{N_{\text{p}}} \ln \phi_{\text{p}} + (1 - \phi_{\text{p}}) \ln(1 - \phi_{\text{p}}) + \chi \phi_{\text{p}} (1 - \phi_{\text{p}}) \right]$$

The first two terms describe the entropic contributions, while the third term describes the energetic contributions contained in χ . As χ grows, the energetic contributions begin to rival the entropic contributions, and at a critical point $\chi_{\mathcal{O}}$ the system becomes energetically unstable due to the energetic contributions outweighing the entropic ones. At this point, the system

phase-separates into two phases, which together are more energetically favorable than a single phase of polymer dissolved in solvent.⁴

1.1.2. Phase Diagram. For a polymer solution, the binodal boundary is determined by finding the two equilibrium concentrations $\phi_{\rm p,e1} \leq \phi_{\rm p,e2}$ of $\Delta F_{\rm mix/site}$ as a function of temperature (T). These concentrations are found at the two local free energy minima, i.e., where $\frac{\partial}{\partial \phi_{\rm n}} \Delta F_{\rm mix/site} = 0$ and

 $\frac{\partial^2}{\partial \phi_p^2} \Delta F_{\text{mix/site}} > 0 \text{ (Figure 1a)}. \text{ The relationships of equilibrium concentration as a function of temperature } \phi_{\text{p,e1}}(T) \text{ and } \phi_{\text{p,e2}}(T) \text{ can then be used to construct the binodal phase boundary on a plot of } T \text{ vs } \phi_{\text{p}}. \text{ The interaction parameter } \chi \text{ can then be determined by calculating the common tangent line connecting } \frac{\partial}{\partial \phi_p} \Delta F_{\text{mix/site}}|_{\phi_p = \phi_{\text{p,e1}}} = \frac{\partial}{\partial \phi_p} \Delta F_{\text{mix/site}}|_{\phi_p = \phi_{\text{p,e2}}} \text{ and solving for } \chi_{\text{binodal}}.$

By solving $\frac{\partial^2}{\partial \phi_p^2} \Delta F_{\text{mix/site}} = 0$ for $\chi = \chi_{\text{spinodal}}$ one can then determine the spinodal boundary as a function of T and ϕ_p as follows. The interaction parameter χ can be expressed as a function of temperature through $\chi(T) \cong A + \frac{B}{T}$, where A and B can be experimentally determined through a plethora of different techniques. The solution to $\frac{\partial^2}{\partial \phi_p^2} \Delta F_{\text{mix/site}} = 0$ in terms of χ_{spinodal} can be rewritten in terms of T and the experimentally determined T and T an

$$T_{\text{spinodal}} = \frac{B}{\frac{1}{2}[1/(N_{\text{p}}\phi_{\text{p}}) + 1/(1 - \phi_{\text{p}})] - A}$$

Note that a polymer solution will only phase-separate above a critical concentration, $\phi_{\rm p} \geq \phi_{\rm c}$, which can be calculated from $\frac{\partial}{\partial \phi_{\rm p}} \chi_{\rm spinodal} = 0 = \frac{1}{2} \bigg[-\frac{1}{N_{\rm p} \phi_{\rm c}^2} + \frac{1}{(1-\phi_{\rm c})^2} \bigg].$ For a polymer solution, that critical concentration is $\phi_{\rm c} = \frac{1}{\sqrt{N_{\rm p}}+1}$. As $N_{\rm p}$ is generally very large, $\phi_{\rm c} \cong \frac{1}{\sqrt{N_{\rm p}}}$ and thus scales with the size of the polymer. If the polymer is small, the critical concentration for phase separation will be higher, and vice versa. This theoretical result is often—but not always—reflected in experimental data, as will be discussed in section 1.2.

Using the critical concentration, the critical temperature $T_{\rm c}$ at which the solution will phase-separate can be predicted. Substituting $\phi_{\rm c}$ into $\chi_{\rm spinodal}$, one gets the critical interaction parameter $\chi_{\rm c,spinodal} = \frac{1}{2} \bigg(\frac{1}{\sqrt{N_{\rm p}}} + 1 \bigg)^2$, which when expressed as $\chi(T)_{\rm c,spinodal} = A + \frac{B}{T_{\rm c}}$ can be rearranged to define the critical temperature $T_{\rm c} = \frac{B}{\frac{1}{2}[(1/\sqrt{N_{\rm p}})+1]^2-A}$.

The phase diagram is an incredibly useful tool for understanding the behavior of polymer solutions. It allows one to predict the temperature at which a polymer solution of a given concentration will phase-separate or, conversely, at which concentration a polymer solution at a given temperature will phase-separate. In practice, for a biopolymer in solution, the higher equilibrium concentration $\phi_{p,e2}$ describes its concentration in the dense condensate phase, while the dilute, lower equilibrium concentration $\phi_{p,e1}$ corresponds to the concentration of individual biomolecules remaining in solution after

phase separation has occurred. The following sections describe how this theoretical understanding of the balance between entropic and energetic contributions that drive liquid—liquid phase separation has been applied to understand the behavior of synthetic and biological systems that exhibit LLPS.

1.1.3. Flory—Huggins Description of UCST/LCST Behavior. Polymers exhibit two types of phase behavior: upper critical solution temperature (UCST) and lower critical solution temperature (LCST) phase behavior (Figure 1b). Polymers that transition at all $T \le T_c$ exhibit UCST behavior, where the T_c is the highest temperature at which the polymer will phaseseparate. UCST behavior can be directly predicted by and modeled by the Flory-Huggins theory described above. In general, from the experimentally determined $\chi \approx A + \frac{B}{T}$, if B >0, then χ decreases with increasing temperature and the system exhibits UCST behavior. From Flory-Huggins theory, we see that UCST behavior typically arises from the energetics of polymer-polymer, polymer-solvent, and solvent-solvent interactions outweighing the entropic contributions to solubility.^{8,9} Polymers that transition at all $T \ge T_c$ exhibit LCST behavior—the T_c is the lowest temperature at which the polymer will phase-separate. In general, if B < 0, then χ increases with increasing temperature and the system exhibits LCST behavior. This phase separation is driven by the increase in entropy of the system resulting from the expulsion and release of water molecules from the polymer molecules' hydration shells upon condensation.5,8

1.1.3.1. Extensions of Flory—Huggins Theory. Modeling LCST behavior has been done by extending the Flory—Huggins lattice-based theory described above to a liquid-lattice model that incorporates vacant sites and thus the compressibility of the mixture. This extension is important, as it has been recognized that LCST behavior is correlated with variable density within the system, a modular parameter that is not explicitly included in the original formulation of the Flory—Huggins theory. Specifically, the expulsion of solvent from the dense polymer phase changes the density within the dense phase condensate. Although UCST phase behavior follows more readily from Flory—Huggins theory and is somewhat more intuitive, LCST behavior of polymers has been significantly better characterized experimentally, and thus we will discuss it first.

Beyond extensions to accommodate LCST phase transitions, many subsequent improvements in theoretical descriptions of polymers have made the Flory-Huggins predictions more accurate. Overbeek and Voorn expanded Flory-Huggins theory to describe complex coacervation by considering the mixing of polyelectrolytes and their electrostatic interactions 11,12 and Koningsveld and Staverman expanded Flory-Huggins theory from a two-component homopolymer solution to encompass multicomponent polymer solutions¹³—two expansions which are integral for studying how proteins, large and complex polyelectrolytes, behave in highly heterogeneous multicomponent protein condensates. 11 For example, Lin et al. applied polymer physics theory that accounted for electrostatic interactions in polyampholyte solutions to predict the phase behavior of the DDX4 nuage protein (described later in this paper). 14 Other corrections to Flory-Huggins theory help reconcile differences between general mean-field theory and experimental results as a result of scaling factors 15,16 or fluctuations in the concentrations of phase-separated polymers around the critical demixing point. Further discussion on the

physics of biological phase separation has been covered in other excellent reviews. $^{5,18,19}\,$

1.2. Liquid—**Liquid Phase Separations** *in Vitro*. The following section describes synthetic macromolecules that exhibit LCST and UCST phase behavior and discuss the various parameters that influence their phase behavior.

1.2.1. Synthetic Polymers That Exhibit LCST and UCST Phase Behavior in Aqueous Solvents. Poly(N-isopropylacrylamide) (PNIPAM) is a canonical—and extensively studied example of an LCST synthetic polymer. Aqueous solutions of PNIPAM phase-separate as the solution is heated up to its T_c (~31-33 °C), with the interesting property that this LCST phase transition is independent of the concentration of PNIPAM or the molecular weight of the polymer.²⁰ This lack of dependence of the T_c on these two parameters indicates that the entropic effects of hydrophobic hydration of the polymer and subsequent release of bound water from the polymer chains on phase separation are the primary forces that drive phase separation of PNIPAM. The concentration of PNIPAM within the dense phase is 0.4 g/mL, and this concentration of the dense phase is also independent of the aqueous PNIPAM concentration in the single phase prior to phase separation.²⁰

Poly(oligoethylene glycol methyl ether methacrylate) (PO-EGMA) is a methacrylate polymer with oligo(ethylene glycol) (OEG) side chains appended to the methacrylate repeat unit. Like PNIPAM, POEGMA exhibits LCST behavior in aqueous solution. The T_c at which POEGMA phase-separates is highly dependent on the length of the OEG side chains, 21 with POEGMA polymers with OEG repeats with length 2-10 EG units in the side chain exhibiting T_c ranging from 26 to 90 °C.²¹ In the case of POEGMA, the Helmholtz free energy of phase transition is based on the balance between the hydrophobic methacrylate backbone and the hydrophilic OEG side chains. A molecular dynamics study of POEGMA found that, below the T_{c} POEGMA chains in an aqueous solvent are solubilized through hydrophobic hydration around the OEG side chains forming a "cage" around the backbone, but as the temperature is increased, the bound water molecules are released, increasing the entropy through reduction in water-ordering around the polymer and in turn driving its phase transition.²² With this understanding, one finds that the T_c of POEGMA increases as the OEG chains are elongated; however, the T_c of POEGMA does not change significantly with increasing polymerization of OEGMA blocks.²³ In addition, the LCST of POEGMA increases only slightly with a decrease in concentration.²³

Interestingly, POEGMA exhibits a UCST phase transition in aliphatic alcohols. The UCST phase separation $T_{\rm c}$ is a function of the POEGMA molecular weight, concentration, OEG end group, and structure of the alcohol. Increased alcohol chain length increases the UCST cloud point, while increasingly hydrophobic OEG end group modifications decrease the UCST cloud point in alcohol and the LCST cloud point in water. The dependence of UCST on OEG end group and solvent alcohol structure highlights the importance of molecular interactions between the polymer and solvent on UCST behavior.

Poly(ethylene glycol) (PEG), a workhorse polymer with myriad applications in many fields, when dissolved in water demonstrates "closed loop" LCST and UCST phase behavior. A solution of PEG in water first undergoes an LCST transition by demixing of a single soluble phase into two immiscible phases. As the temperature is raised further, PEG undergoes a UCST phase transition, becoming soluble again. This closed loop phase behavior has been attributed to intermolecular

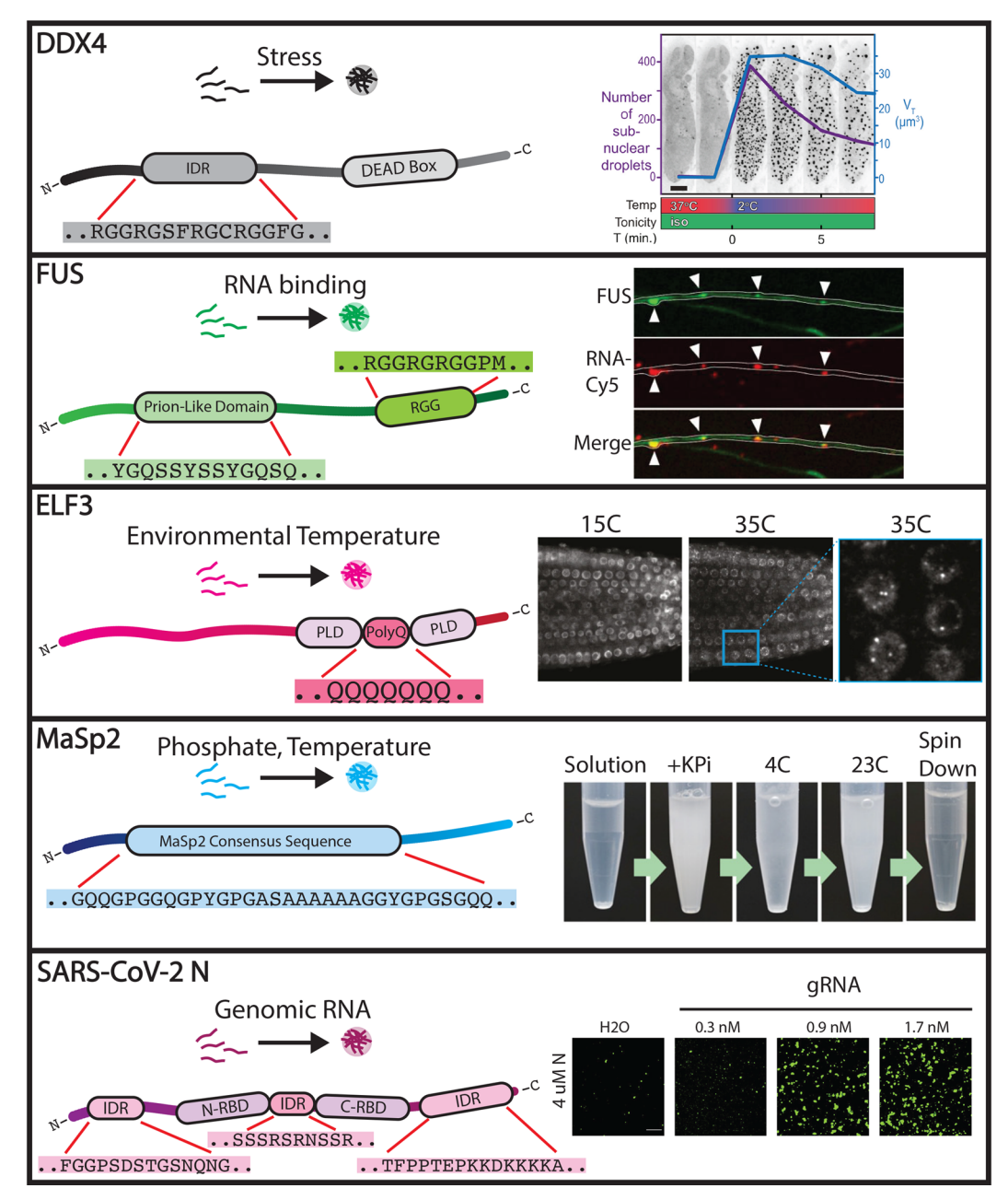


Figure 2. Phase separation of proteins. Intrinsically disordered proteins, selected sequence portions of the relevant disordered regions, and their phase separation behavior. DDX4 contains a large N-terminal intrinsically disordered region (IDR) and a DEAD Box RNA Helicase consensus sequence. In response to a temperature shock, DDX4 droplets rapidly condense in HeLa cells. Adapted with permission from Nott et al. ⁴⁴ Copyright 2015 Elsevier. FUS contains a prion-like domain (PLD) and an RGG binding domain. FUS selectively phase-separates with RNA. Adapted with permission from St George-Hyslop et al. ⁶⁹ Copyright 2018 Elsevier. ELF contains a poly-Q domain within a larger PLD—the pol-Q domain is integral for phase separation. Upon temperature increase, ELF3 phase-separates to form intracellular granules. Adapted with permission from Springer: Nature, Jung et al. (2020). ⁴⁵ The MaSp2 spidroin contains an aliphatic consensus sequence enriched in G, Q, and A. Upon addition of phosphate, MaSp2 phase-separates—these condensates are then soluble at low temperatures and condensed at high temperatures. Adapted with permission from Malay et al. ⁵⁶ Copyright 2017 PLOS One. The N protein of the SARS-CoV-2 virus phase-separates with viral genomic RNA. Adapted with permission from Iserman et al. ⁵⁷ Copyright 2020 Elsevier.

interactions that depend on a specific orientation—in the case of PEG, the hydrogen bonds between the end groups. The LCST phase behavior of PEG is highly dependent on both the MW of the polymer and the salt concentration of the water, decreasing from 172 down to 101 °C with increasing MW and salt concentration of the polymer. The UCST cloud point has been found to increase with increasing MW of the polymer. These results imply that the entropic drivers for phase transition

of PEG lie in the unfavorable energetic interactions between the PEG chains and water at high temperatures.

In general, the UCST phase behavior of polymers is strongly dependent on energetic interactions, such as hydrogen bonding or Coulombic interactions between functional groups in the polymer and the solvent. For example, zwitterionic copolymers of poly(ethylene glycol) (PEG) and sulfobetaine or sulfabetaine methacrylates exhibit UCST phase behavior in water or saline medium based on the absence or presence of an oxygen atom

within non-PEG polymer blocks. Specifically, polymers with polysulfobetaine methacrylate blocks exhibited UCST behavior only in water, while polymers with polysulfabetaine methacrylate blocks exhibited UCST behavior only in saline solution. Another example is poly(N-acryloylglycinamide) (PNAGA), which displays UCST phase behavior in water. The introduction of even a trace of ionizable groups into the polymer, however, abolishes UCST behavior, while adding counterions in the form of salt can counteract these effects by shielding the ionizable groups in the polymer from the solvent and short-range intermolecular interactions between ionizable groups in the polymer.

1.3. Phase Separation of Proteins. 1.3.1. Introduction to Phase-Separating Proteins. From this understanding of canonical phase separation, we proceed to the phase separation of proteins. Over the past decade, many newly described intracellular condensates that form through phase separation have been reported in different biological systems and have been the subject of multiple studies that further our knowledge of their formation and function. The nucleolus and Cajal bodies were the first intracellular condensates discovered almost a century ago, ^{28,29} but their liquid-like nature was only suggested in 2005³⁰ and experimentally shown in 2009.³¹ The list of intracellular condensates has greatly expanded since then. 30,32,33 For instance, nuclear speckles are membrane-less nuclear bodies, while stress granules (SGs), processing bodies (PB),³⁴ germ granules, and the centriole are examples of cytoplasmic condensates. 35,36

Many naturally occurring proteins that phase-separate contain intrinsically disordered regions, IDRs, comprising stretches of amino acids which are not predicted to fold into a specific 3D structure. TDRs within IDPs contain distributed weakly interacting motifs that provide the driving force in the formation of condensates of an IDP. Bioinformatic searches of eukaryotic genomes have predicted extensive IDRs in diverse proteins, and these phase-separated protein condensates of IDPs play myriad roles in physiology, from controlling cellular noise and modulating gene expression when phase-separated with RNA to catalyzing biochemical reactions by bringing dilute proteins in close proximity. The following sections describe a few examples of proteins with IDRs that have been shown to undergo liquid—liquid phase separation *in vivo* and provide a brief description of the impact of electrostatic interactions on protein—protein and protein—RNA phase separation.

1.3.2. Proteins with Intrinsically Disordered Regions (IDRs). The DDX4 family of proteins exhibit phase-separation behavior mediated by IDRs (Figure 2). These proteins form membraneless organelles in a variety of organisms, such as the nuage in mammals⁴⁴ and P-granules in *C. elegans*. Proteins in the DDX4 family contain an RNA helicase sequence flanked by long N- and C-terminal IDRs, containing 8–10 amino acid repeats of alternating charge. The positively charged regions are rich in FG, GF, RG, and GR amino acid motifs. Indeed, DDX4 tagged with YFP exhibits UCST behavior—at high temperatures, DDX4 condensates solubilize, while, at lower temperatures, the condensates reform as a dense, water immiscible phase.

Many proteins associated with diseases have also been shown to phase-separate, ^{49–53} implying a potential connection between phase separation and disease. One of the most extensively studied examples is the Fused in Sarcoma (FUS) protein that is involved in many RNA-related activities such as transcription, splicing, and transport in the cell⁵⁴ (Figure 2). FUS exhibits LLPS within the cell and has a low-complexity IDR rich in S, Y,

G, and Q residues⁴⁹ and a region rich in RGG repeats⁵⁰ that binds RNA. Recent studies have shown that interand intramolecular interactions between the IDR and RGG residues are important for the UCST phase behavior exhibited by FUS⁵⁴ and that FUS preferentially phase-separates at high salt concentration and in the presence of RNA.⁴⁹

The *in vivo* LLPS of proteins is not only restricted to UCST phase behavior. A prion-like domain in the protein Early Flowering 3 (ELF3) drives LCST phase separation of an "evening" complex in *Arabidopsis thaliana* composed of ELF3, ELF4, and LUX, a transcription factor⁴⁵ (Figure 2). The LCST phase separation of this complex allows transcription of genes driving the flowering of the plant, thus acting as a thermosensor for elevated temperature. This LLPS is facilitated by a polyglutamine repeat embedded in a prion-like domain in ELF3; deletion of this poly-Q repeat abolishes the phase separation behavior and temperature responsiveness of the evening complex.⁴⁵

The formation of spider silk as well involves LCST phase transitions of spidrion silk precursors ⁵⁵ (Figure 2). The dragline silk protein major ampullate spidroin 2 (MaSp2) contains an amphiphilic tandem repeat domain rich in glutamine, alanine, and glycine residues, and solutions of MaSp2 undergo LCST phase separation into a dense condensate upon the introduction of phosphate ions. ^{55,56} This condensate then rapidly assembles into spider silk fibrils upon acidification. In essence, the LLPS of spidroin precursors into a dense condensate facilitates the creation of fibrils, underscoring the significance of phase separation in the processing of silk into fibers.

The viral SARS-CoV-2 N protein undergoes LCST phase separation as part of the capsid packaging process, preferentially forming a condensate with its own viral genome RNA and excluding the rest of the RNA within the cell^{57,58} (Figure 2). The N protein structure includes two RNA-binding domains (RBDs), an N-terminal RBD, and a C-terminal RBD that also acts as a dimerization domain, a disordered serine-rich linker, and N- and C-terminal IDRs. 57,58 Phosphorylation of the serinerich linker drives N protein-RNA assembly from a gel-like state to one reminiscent of LLPS. 58 Indeed, the phase separation of N protein together with the SARS-CoV-2 genomic RNA increases in efficiency as the temperature rises from a normal body temperature of 37 °C to more febrile temperatures of 40–45 °C. 57 The LCST phase behavior of the N protein may indicate that the SARS-CoV-2 virus takes advantage of fever resulting from a host immune response to increase the efficiency of functions associated with its replication.

1.3.3. Electrostatic Interactions in Biological LLPS. A feature common to proteins which undergo UCST phase transitions is the presence of charged residues (e.g., lysine, arginine) that facilitate the electrostatic intermolecular interactions that are implicated in UCST phase behavior. The patterning of these residues affects the structure and compactness of phase-separated proteins, ⁵⁹ while the overall distribution of positive and negative charge along a protein's amino acid sequence may be the driving force for LLPS, rather than the specific protein sequence. ⁶⁰ Further reading on the subject can be found in an excellent review by Bianchi et al. ⁶¹

These electrostatic interactions also underlie the influence of RNA on phase-separating protein—RNA condensates. Many proteins, including the DDX4, FUS, and SARS-CoV-2 N proteins mentioned above, interact with RNA when they phase-separate to form ribonucleoprotein (RNP) granules—membrane-less organelles rich in protein and RNA that have myriad

roles in biological systems. A slew of recent research has demonstrated that, beyond the constituent proteins, RNA also plays a key role in modulating the structure and phase separation behavior of these RNP granules. RNA has been shown to determine the size of intracellular condensates, wherein a larger RNA:protein ratio led to smaller yet more numerous RNP granules. 62 This result agrees with numerous studies demonstrating that RNA is able to buffer and even dissolve RNP granules. At low RNA concentrations, the RNA molecules drive nucleation and assembly of protein-RNA condensates; however, as the RNA concentration increases further, the condensates begin to dissolve. 63 This phenomenon is rooted in the balance between short- and long-range electrostatic and sequence-encoded cation-pi interactions.⁶⁴ This has a particularly poignant role in the formation of condensates by proteins encoding prion-like domains (PLDs); PLD-containing proteins which undergo phase separation such as FUS and TDP43 have been implicated in a number of neurodegenerative diseases. 65,66 Maharana et al. showed that high nuclear concentrations of RNA prevent aberrant phase separation of proteins containing PLDs but lower concentrations of RNA mislocalized to the cytoplasm actually serve to nucleate aberrant intracellular condensates. Further details on the role of RNA in LLPS can be found in an excellent and thorough review on the subject by Roden and Gladfelter.6

2. METHODS TO STUDY LIQUID—LIQUID PHASE SEPARATION IN PROTEINS

In this section, we give an overview of the experimental and computational techniques used to quantify and study the phase separation of proteins and refer the reader to many other excellent reviews that have been written covering these techniques in more details.¹¹

2.1. Experimental Methods. The phase diagram of protein—nucleic acid assemblies in solution has been mapped as a function of temperature, pH, concentration, salt type and concentration, cosolutes, and the volume excluded by other macromolecules. ^{3,44,49,60,70–73} Droplets that form through LLPS have been directly imaged—and studied—in live cells by fluorescence microscopy, high speed atomic force microscopy (AFM), and fluorescence recovery after photobleaching (FRAP). ⁷⁴ FRAP, in particular, is a very useful technique to study the molecular dynamics and mobility of phase-separated domains and has been used to monitor droplet maturation and investigate the diffusion of macromolecules in LLPS droplets. ^{74–76}

NMR spectroscopy has also been used to investigate how different domains of a protein contribute to the formation of phase-separated condensates of an IDP. ^{49,52,77} The lack of persistent secondary and tertiary structure found in IDPs and IDRs that exhibit LLPS is not an impediment to NMR studies, in contrast to X-ray crystallography, and enables NMR to provide information on the local structure of proteins undergoing LLPS and information about the inter- and intramolecular interactions that drive LLPS. ⁷⁸ For instance, measurements of H1-exchange rate, chemical shifts, and residual dipolar coupling (RDC) have been used to investigate the transient secondary structural elements of disordered segments ns LLPS domains, ⁷⁹ while paramagnetic relaxation enhancement (PRE) ⁸⁰ and pulse-field gradients (PFGs) have been used to investigate the long-range interactions of IDPs (up to 25 Å). ^{52,54,81–85}

Other structural characterization methods can be combined with NMR analysis to study the phase separation of IDPs. Small

angle X-ray scattering (SAXS) and small angle neutron scattering (SANS) can complement NMR and provide the three-dimensional protein structure. S6-89 Förster resonance energy transfer (FRET) can also provide information on the distance between pairs of fluorescently labeled amino acids in IDPs. Raman spectroscopy has also been used in combination with NMR to characterize the interactions within an IDP condensate. Recently, a method for microrheological measurements of phase-separated coacervates has been developed that uses optical tweezers to determine the elastic modulus, viscosity, and surface tension of a coacervate. This method was used by the Hyman group to characterize phase-separated droplets of the *C. elegans* PGL-3 protein. PI

Differential scanning calorimetry (DSC) is another useful technique which can provide valuable information on the intrinsic disorder of proteins. ⁹² In this technique, the heat capacity difference between the protein solution and a reference is recorded at constant pressure accompanying uniform heating/cooling cycles. DSC can provide accurate analysis of the folding and phase transition of IDPs and partially disordered proteins and facilitates the understanding of their stability and energetic profiles. ^{93–96} DSC is best suited for relatively small and structurally cooperative proteins; the technique is limited in extracting structural information from large, multidomain proteins in which each domain has different structural cooperativities. ⁹²

DSC has also been used with other calorimetric and spectroscopic methods to study LLPS in IDPs. For instance, DSC has been employed with pressure perturbation calorimetry (PPC) and FT-IR to investigate the phase separation behavior of insulin. The has also been used with HNMR to study the water and ion-binding properties of the full transactivation domain (TAD) of p53, an intrinsically disordered domain within the full tumor suppressor protein. Tompa et al. showed that the combination of DSC and NMR can distinguish between IDPs and folded, globular proteins and furthermore can also differentiate between the disordered wild type and ordered, helical mutant variants of the intrinsically disordered TAD peptide portion of the p53 TAD protein. See turbation of the p53 TAD protein.

Electron paramagnetic resonance (EPR) spectroscopy is another magnetic resonance technique similar to NMR in which energy is absorbed by the magnetic moments of unpaired electrons. As unpaired electrons are rare in biological molecules, this technique exhibits very low background signal for *in vivo* imaging. The combination of EPR with site-directed spin labeling (SDSL-EPR) provides a useful technique for the characterization of the structural behavior and dynamics of proteins lacking a well-defined 3D structure (IDPs) under physiological conditions.

Florescence correlation spectroscopy (FCS) is another powerful technique that provides information about small molecular ensembles by measuring the spontaneous fluorescent intensity fluctuations of fluorescent particles. PCS has been frequently used to study biological condensates and soluble aggregates. For instance, Alshareedah et al. incorporated FCC, combined with microrheology and optical tweezer induced droplet fusion, to quantify the viscosity, surface tension, and diffusion of protein—nucleic acid condensates. In another example, Peng et al. used the dual-color fluorescent crosscorrelation spectroscopy (dcFCCS) method to study the formation, size, and growth rate of nanoscale condensates. They also used this method to investigate the binding affinity of molecules within the condensates. Ultrafast-scanning FCC

has also been used to measure second virial coefficients, molecular diffusion, and binodal coexistence curves of *C. elegans* proteins in the presence and absence of RNA. ¹⁰⁶

2.2. Computational Methods. The major limitation of experimental techniques used to characterize the LLPS of macromolecules ¹⁰⁷ is that they cannot provide detailed information on the interactions of components in the complex environment within LLPS condensates, especially the conformational ensembles and the dynamics of disordered proteins at the molecular level. Theoretical and computational tools can provide complementary information about conformational ensembles of macromolecules across short length and time scales that are not accessible by experimental methods and access to the structural details of condensates that are difficult to obtain by experimental methods, and information about the thermodynamics and kinetics of phase separation. ^{108–112}

The majority of computational studies on IDPs and proteins containing IDRs employ coarse-grained (CG) models in which individual proteins are treated as colloidal particles based on Debye-Hückel electrostatics and empirical contact potentials. 113-115 CG methods are able to qualitatively analyze the sequence-dependent properties of IDP/IDRs and in some instances can provide results in close agreement with experimental results. 116 CG methods have also been used to calculate the phase diagrams of coexisting systems such as FUS and the DEAD-box helicase protein LAF-1. 85 CG methods have been used to relate protein sequence to its phase-separation behavior by quantifying the correlation between the temperature of chain collapse, self-associating temperature, and the critical temperature for phase separation in dilute solution. 85 As summarized by Paloni et al., 117 modeling the organization of membrane-less organelles and describing the role of phosphorylation on LLPS are other examples of CG simulations that have expanded our knowledge of LLPS.

Molecular dynamics (MD) and Monte Carlo (MC) simulations are two other computational methods that are useful for studying LLPS at the molecular level. 118,119 MD and MC simulations are based on a force-field energy function that includes both bonded and nonbonded interactions and thus have the advantage of being able to account for detailed intermolecular correlations. MD has the ability to predict dynamic properties such as nucleation kinetics and transport coefficients and also provides a direct computational route to investigate structurally disordered states at the atomic level, paving the way for elucidation of the structural dynamics of folded, disordered, and partially disordered proteins. 120,121 The quality of MD simulations, however, is highly dependent upon an accurate physical force-field model. The MC methods overcome this problem by utilizing discontinuous force-fields such as particle swaps in multiphase systems 122 summarized in ref 110.

3. FROM LLPS PRINCIPLES TO APPLICATIONS

As the body of research on LLPS in biology grows in scope and significance, there has been a simultaneous push to understanding the phase behavior in bioinspired materials. Diverse artificial polypeptides have been shown to exhibit LCST and UCST phase behavior. 123 This phase behavior has been typically found in repetitive polypeptides with high levels of intrinsic disorder, termed artificial intrinsically disordered proteins (A-IDPs). The canonical LCST exhibiting IDPs are made out of repeat units Valine-Proline-Glycine-Valine-Glycine and exhibit LCST phase transitions at $\sim\!30~^{\circ}\text{C}.^{124,125}$ This (VPGVG), motif

was originally derived from the observation that the motif recurs multiple times and is highly conserved within the hydrophobic region of the tropoelastin protein across all species that produce it. Tropoelastin is a protein with a high level of structural disorder that in humans polymerizes to form elastin; the inspiration of polymers of this class of peptide motif from elastin has led them to be named elastin-like polypeptides (ELPs).

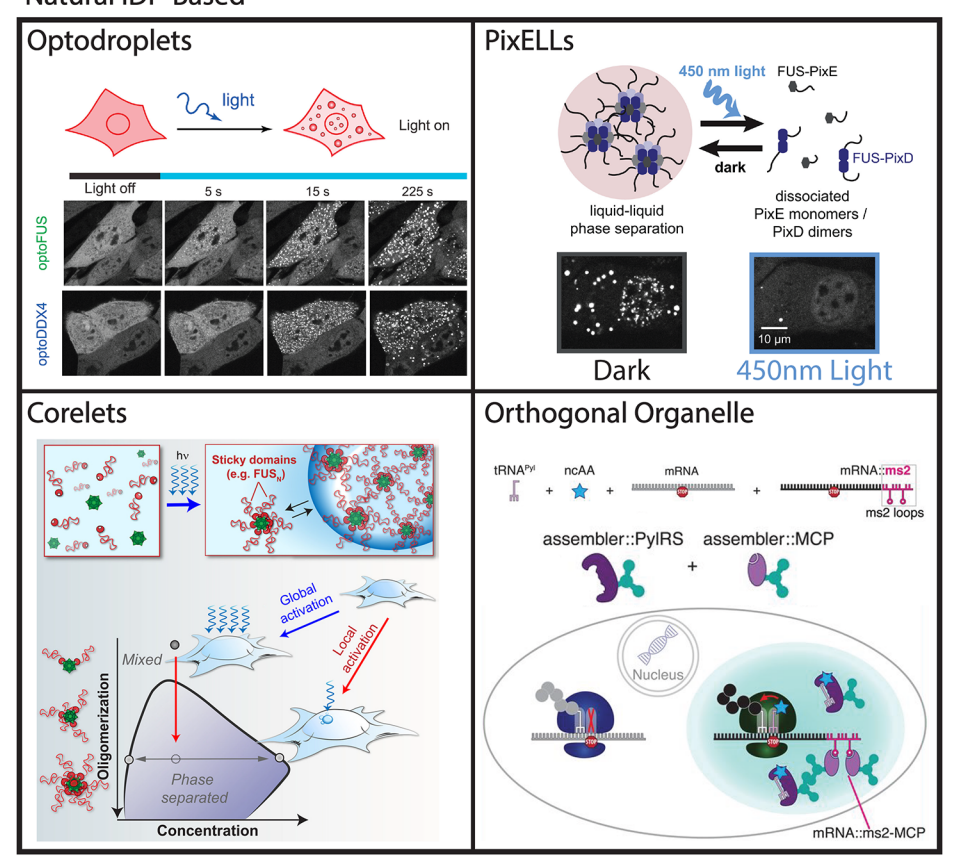
For a long time, there was a dogmatic belief that the fourth position in the pentapeptide repeat was the only position that is tolerant to substitution without abolishing the LCST phase behavior of ELPs. This led to the generalization of this motif to (Valine-Proline-Glycine-Xaa-Glycine),, where Xaa is any amino acid except proline. The T_c of the polymer can be tuned by modulating the hydrophobicity or hydrophilicity of the guest residue Xaa. ¹²³ In addition, there was a persistent notion that the VPGXG motif uniquely conferred LCST phase behavior to peptide polymers. That this notion was simply dogma was suggested by the observation that (IPGVG),, with a valine to isoleucine substitution at the first residue of the repeat unit, departs from the canonical VPGXG sequence yet still exhibits LCST phase behavior.

Further advances in multiplexed IDP gene synthesis laid the groundwork for the discovery of new phase-separating IDP sequences that diverged from the canonical (VPGXG)_n motif. Overlap extension rolling circle amplification (OERCA), a novel method that uses rolling circle amplification to multiplex the assembly of repetitive genes that encode for A-IDP oligomers ranging in size from 10 repeats to over 80, was used to generate a library of nine A-IDP genes with various alanine insertions and substitutions in the (VPGVG)_n motif. Four new motifs—(AVPGVG)_n, (VPAGVG)_n, (VPGAVG)_n, and (VPGVAG)_n—were discovered that also undergo phase separation, confirming that there exists a large A-IDP sequence space of LCST phase behavior beyond the canonical (VPGXG)_n motif.

This sequence space has since been extensively explored through the generation of even more complex A-IDPs with varying repeats of the form P- X_n -G, n = 0-4, separated by 3-15 various amino acid residues.³ This novel sequence heuristic has given rise to a plethora of phase-separating A-IDPs which undergo both LCST and UCST phase transitions. Identified LCST phase-separating A-IDPs were shown to demonstrate a range of hysteretic phase separation behaviors, further building on the characterization of this large sequence space and demonstrating the wide functionality of protein phase separation. ¹²⁷ Identified UCST phase-separating A-IDPs are based on a GGRPSDSYGAPGGGN core sequence and are inspired by resilin, a disordered protein found in insect wings, earning them the name resilin-like polypeptides (RLPs).^{3,128}

3.1. Phase Behavior in Artificial IDPs. Similar to naturally occurring IDPs that exhibit LCST and UCST phase behavior, A-IDPs based on ELPs and RLPs exhibit phase behavior and are structurally disordered. Despite the extreme simplicity of these systems—composed as they are of only a few amino acids in a repetitive arrangement—they recapitulate notable features of IDPs found in nature. RLPs, notably, share the same prevalence of glycine, arginine, and tyrosine residues as many IDPs mentioned in Figure 2. Many variants of RLPs also contain glutamine, an amino acid highly prevalent in natural IDPs. In fact, A-IDPs have been engineered which form intracellular condensates with tunable $C_{\rm sat}$ size, and formation temperatures in vivo and subsequently increase enzymatic conversion of a desired reaction within the intracellular condensate, 47 two

Natural IDP-Based



De Novo IDP-Based

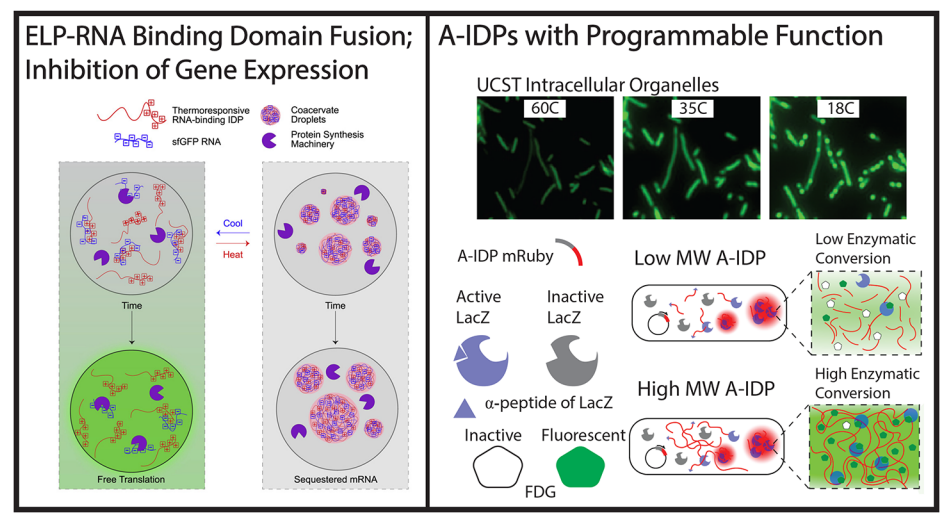


Figure 3. Engineered intracellular condensates. Engineered intracellular condensates can be split into two systems—those based on natural IDPs and those based on de novo IDPs. Systems based on natural IDPs incorporate oligomerization domains that facilitate the spatiotemporal control of condensates and include the optoDroplet system utilizing light-induced Cry2 oligomerization (adapted from Shin et al. ¹³¹), the light-disassembling PixELLs system based on PixE and PixD (reprinted from Dine et al. ¹³⁴), the Corelets system based on a ferritin core and iLID/SspB optical switch (adapted from Bracha et al. ¹³²), and a membrane-less organelle used for orthogonal translation, containing kinesin-targeting domains for spatial partitioning at microtubule plus ends (from Reinkemeier et al. ¹³⁸). De Novo IDP systems are engineered with fully exogenous condensates, including ELPs fused to RNA-binding peptides for temperature-dependent sequestration of RNA from translation machinery in proto-cells (reprinted from Simon et al. ¹³⁷), and a split β-galactosidase system with acceleration of enzymatic activity in RLP condensates as demonstrated in *E. coli* (adapted from Dzuricky et al. ⁴⁷).

important properties of naturally occurring IDPs that phaseseparate *in vivo*. ^{46,129} Because the phase behavior of these A-IDPs can be tuned by systematic changes in their sequence and MW, they offer a potentially useful system to tease out the molecular grammar¹³⁰—how residues, motifs, and IDP blocks come together to impart phase behavior—of phase behavior in far more structurally complex and heterogeneous native IDPs such as FUS.

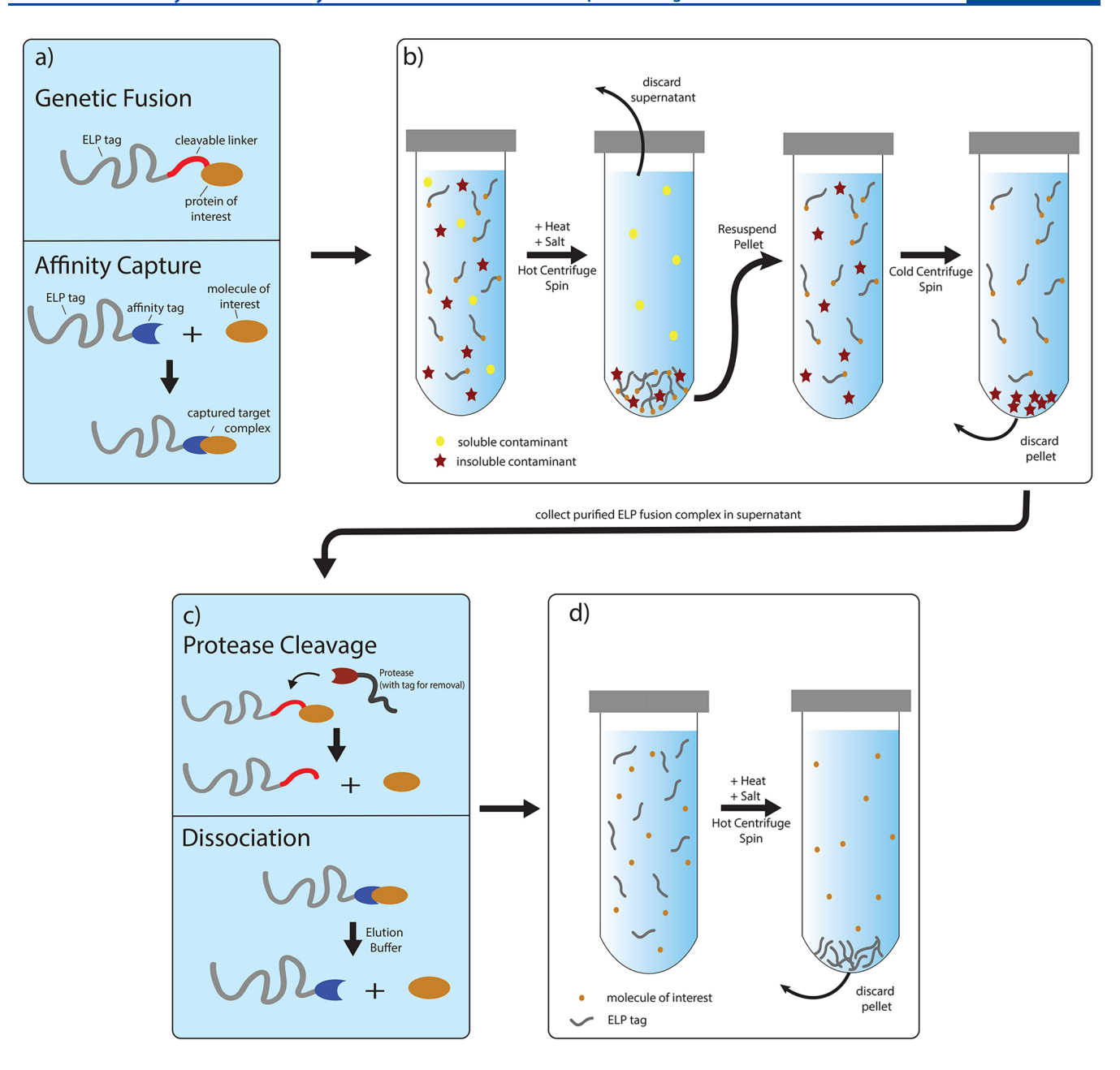


Figure 4. LLPS-mediated purification strategies using ELP fusions. (a) Strategies for linkage of the desired target to a phase-separating peptide by either genetic fusion to ELP with an intermediate cleavable linker or affinity capture with an ELP-binding partner fusion. (b) Steps in the inverse transition cycle (ITC) allow for the sequential removal of soluble and insoluble contaminants from cellular lysate containing the desired molecule. (c) Removal of the ELP tag by protease cleavage in the genetic fusion strategy or by elution-mediated dissociation in the affinity capture strategy. (d) A final LCST transition of ELP and subsequent hot spin yields the soluble target with high purity.

A-IDPs that undergo LLPS have found myriad applications across diverse fields. Engineering of such systems relies on knowledge of the factors that affect their LLPS. Because of their simplicity, the phase diagram of repetitive A-IDPs can be rationally optimized for an application by modulating their genetically encodable molecular parameters—sequence, composition, and MW—that dictate their phase behavior. As ELPs are among the best characterized A-IDPs, they have largely monopolized several areas in which IDPs find applications.

In the following sections, we give an overview of applications where A-IDPs that undergo LLPS have found use. These include the control of cellular processes (3.1.1), biomolecule capture

and purification (3.1.2), drug delivery (3.1.3), and the hierarchical self-assembly of macromolecular materials (3.1.4).

3.1.1. Control of Intracellular Condensates. Engineering cellular condensates has great potential for the control of processes that are regulated by condensates and for treatment of diseases that are caused by dysregulation of condensate formation. Due to the relative youth of this field, most recent efforts have been focused on modulating and understanding the behavior of native intracellular liquid phases under various conditions. The understanding accrued from these studies should, however, allow rational design of bespoke condensates in the future. Even at this early stage, there are now extant examples in which artificial condensates have been designed de

novo and used for molecular sequestration, for translation, or as reaction crucibles in a cell-like environment—commonly called protocells—and in live cells.

The Brangwynne group has developed several optically controlled protein tools that facilitate the interrogation of phase boundaries and condensate function in eukaryotic cells. The blue-light-inducible Cry2 oligomerization domain from Arabidopsis thaliana was fused to IDRs of native condensates to create what is termed the optoDroplet system, which accesses a range of liquid and solid-like states depending on levels of supersaturation 131 (Figure 3). A next generation system dubbed Corelets (Figure 3) was developed using a "core" composed of the 24-mer ferritin complex and the light-inducible interaction partners iLID and SspB, 132 in which ferritin monomers were fused to iLID and the native IDR of interest was fused to SspB. Both systems give researchers spatiotemporal control over condensate formation in cells by initiating the intermolecular interactions that drive condensate formation with light. As optoDroplets are prone to irreversible aggregation and gelation, they have largely been used to investigate disease states associated with gel-like condensates, while more reversible Corelets have been used to precisely map phase boundaries in living cells. 133 A third optical system known as PixELLs (Figure 3) uses a protein oligomerization pair that dissolves upon illumination with light and reassociates in the dark, so that stimulation with blue light dissolves the protein dense coacervate phase in a two-phase system and the removal of light allows LLPS to occur.¹³⁴ Finally, dCas9 fused to lightactivated IDRs and guide RNA can localize condensates to specific regions of the genome in response to stimulation by light as well as restructure chromatin ¹³⁵ (Figure 3).

In these previous examples, exogenous proteins were fused to native IDRs to engineer condensates that are reminiscent of the IDPs they are derived from. In contrast, the de novo engineering of condensates using A-IDPs—which offer more tunability in their phase behavior than native IDPs-offers new opportunities for bottom-up reprogramming of cellular functions via customized functional condensates. In an example of this approach, RLPs—a class of A-IDPs that exhibit UCST phase behavior—were expressed in E. coli and observed to retain reversible temperature-dependent phase separation and phase boundaries that were similar to those observed in vitro (Figure 3). Furthermore, these exogenous condensates could recruit proteins and accelerate the activity of an enzyme, β galactosidase. 47 Temperature control of other processes within cells has also been achieved by fusion of an ELP to signaling proteins. Epidermal growth factor receptor (EGFR) was fused to an ELP by Li et al. to enable dynamic control of receptor clustering and downstream kinase modulation that is triggered by the LCST phase transition of the EGFR-ELP fusion in mammalian cells. 136 Another emerging area of interest involves reversible, phase-transition-triggered sequestration of RNA from the cytoplasm within intracellular condensates for posttranscriptional control of protein expression. An ELP fused to a promiscuous RNA binding domain was leveraged for temperature-tunable inhibition of protein expression by sequestering the RNA from the translational machinery in an in vitro setting¹³⁷ (Figure 3). Finally, in what is perhaps the most complete de novo engineered organelle system to date, Reinkemeier et al. created an orthogonal mRNA translationcapable organelle in mammalian cells by fusing various translation machinery to phase-separating and spatially targeted protein domains (Figure 3). In addition, they selectively

recruited target mRNA transcripts to such organelles via RNA MS2 loops that bind MCP protein domains in the organelles. This allowed them to achieve enhanced efficiency in creating polypeptides with unnatural amino acids within these membrane-less organelles, a feat that is often hampered by cross-talk between native and exogenous translation factors. These studies were all published between 2016 and 2020, demonstrating the youth of this field and the rapid rate at which it is evolving.

3.1.2. LLPS for Purification of Recombinant Proteins. Proteins are typically purified by chromatographic methods, but these methods have issues with scalability, throughput, and cost of stationary phase materials. In comparison, purification of biomolecules via LLPS is readily scalable, rapid, and often achievable with a centrifuge or tangential flow filter and common laboratory supplies. The purification process is conceptually extraordinarily simple—it simply requires a means of selectively separating the moiety of interest into the polymer-rich phase, followed by a method to recover the moiety from the dense phase. Phase-separating polypeptides offer an elegant method of selectively sequestering molecules of interest using fusions to other polypeptides at the genetic level, and thus protein fusions to IDPs with LLPS properties has become an attractive method for recombinant protein purification 139 (Figure 4).

There are two major strategies for the ELP-mediated purification of polymers: direct purification and purification by affinity capture methods. The first method simply requires the gene-level fusion of an ELP to the desired protein and has two constraints—first, that the ELP fusion is expressed as a soluble protein in the expression host and, second, that the fused partner not abolish the LCST phase behavior of the ELP (Figure 4a). After expression, the host cells are lysed and the LCST transition of the ELP fusion is triggered thermally by heating the solution above the T_{cp} of the fusion or isothermally by addition of a kosmotropic salt to depress the $T_{\rm cp}$ below the solution temperature. This causes LCST phase separation of the ELP fusion into a protein-dense phase that contains most of the ELP fusion and a protein-depleted aqueous phase. The ELP fusion can be removed from the protein-depleted phase that contains the bulk of the cellular contaminants by centrifugation or by tangential flow filtration. The dense protein phase is then resuspended in cold buffer to reverse the phase transition and solubilize the ELP fusion (Figure 4b). This process—termed inverse transition cycling (ITC)—can be repeated as many times as is needed to yield increasingly pure protein. We have found that proteins fused to the ELP that are hydrophilic and do not contain significant hydrophobic patches on their surface can be purified to homogeneity with only a few rounds of ITC, whereas more hydrophobic proteins tend to attract contaminants and hence require a greater number of rounds of ITC to attain sufficient purity. At this time, our group has purified >30 proteins by this method and ITC has allowed the purification of a number of refractory proteins. ELP fusions and their purification by ITC are not, however, a panacea, as this methodology only applies to proteins that can be expressed as soluble protein.

In many instances, the final product of interest is the protein sans the ELP tag, and to isolate the protein without the fused ELP, a protease cleavage site can be introduced between the ELP and recombinant protein to enable the cleavage of the ELP tag from the fusion by a protease of interest (Figure 4c). We have developed and used a number of such systems including thrombin, 140 sortase, 141 and self-cleaving inteins. 142 After

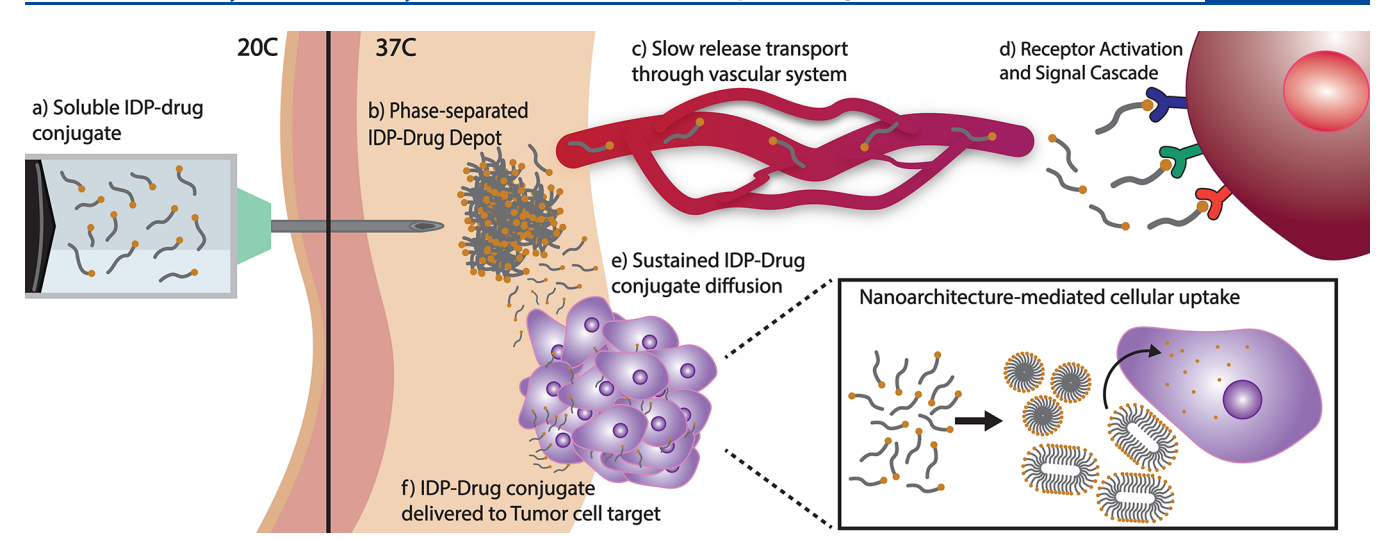


Figure 5. Phase transitions in drug delivery. The LCST transition of ELP-drug conjugates mediates its formation into a variety of molecular assemblies and thus its distribution in the body. (a) IDP-drug conjugates that are soluble at room temperature can transition into (b) phase-separated ELP depots in the body when exposed to body temperature (37 $^{\circ}$ C). These depots slowly release IDP-drug into the bloodstream (c), where they can undergo programmed receptor-mediated targeting (d), or release the conjugate to local tumors (e, f). (Inset) Various nanoparticle architectures using engineered LLPS peptide conjugates have been demonstrated to facilitate drug encapsulation, evade immune detection, and enhance ligand presentation.

cleavage, an additional ITC step can be carried out to separate the cleaved ELP (Figure 4d). Although other phase-separating polypeptides have been used to similar effect, such as an RLP exhibiting a UCST transition, ¹⁴³ and various polyelectrolyte protein—polymer combinations that result in complex coacervation, ¹⁴⁴ ELPs remain by far the most developed system for purification of recombinant proteins.

The second LLPS-mediated purification strategy relies on affinity capture of a target protein by an ELP fusion. This method relies on selective binding between the ELP fusion partner and the target, making selection of binding partner pairs highly important for this application. Unlike direct purification of ELP fusion proteins, affinity capture phase separation is not limited to polypeptide-based targets and can be used to purify any target molecule for which a suitable ligand with high binding affinity and selectivity—preferably one that can be recombinantly synthesized as a fusion with an ELP—exists. Early work by the Chen group used fusions of ELP and protein A in order to capture and purify monoclonal antibodies from hybridoma lysates¹⁴⁵ and later optimized the efficiency and yield by replacing protein A with the smaller Z-domain derived from protein A. 146 The same group also developed a recyclable plasmid purification system based on the affinity of the bacterial metalloregulatory protein MerR for its promoter sequence on the target plasmid. 147 A short list of other peptide affinity tag pairs that have been explored for affinity precipitation include SH3 and proline-rich domains, streptavidin and nanotag-15, and flag peptide and antiflag M2. 148,149 Compared to direct purification of ELP fusion proteins, affinity capture followed by phase separation has the advantage that it does not require the target molecule to be modified by fusion to an ELP, although it requires additional steps that may lower its efficiency.

3.1.3. LLPS and Drug Delivery. Drug delivery systems are designed to increase drug solubility, decrease rate of clearance by the kidneys, and in some cases shield the drug from adverse immune recognition. Polypeptides based on ELPs can impart each of these functions and have the additional benefit of degradation into nontoxic byproducts. For applications in

drug delivery, polymers that undergo LLPS have been leveraged to modulate the pharmacokinetics and *in vivo* biodistribution of drugs. In the two most common embodiments of LLPS for drug delivery, phase separation is used either to control the formation of drug depots within the body for sustained release of the drug or to engineer functional particles of defined size and architecture that sequester drug and have extended blood circulation.

Drugs can be attached to an ELP by several methods. Genetically encodable peptide and protein drugs can be fused to an ELP at the gene level, whereas small molecule drugs can be chemically conjugated to the ELP. The design of ELPs as drug carriers requires a systematic approach to optimization of guest residues and molecular weight to tune the transition temperature for its intended application with the additional caveat that the attachment of a drug can alter the phase diagram of the ELP, 152 which must hence also be taken into account in the ELP optimization process.

Perhaps the most straightforward LLPS application in drug delivery relies on the LCST transition from room temperature to body temperature to create an injectable depot for sustained release of a peptide or protein drug fused to an ELP (Figure 5a,b). In this design, an ELP is fused to a drug that, upon subcutaneous injection, forms an insoluble depot at the site of injection but that dissolves over time at a predictable rate with zero order kinetics and thereby releases the ELP fusion into circulation (Figure 5c,d). While they have been explored for a number of applications, 153,154 this approach is especially useful for treatment of diseases that require a baseline dose of the drug at all times—type 2 diabetes is perhaps one of best exemplars of this need. To this end, depots formed by ELP fusions to peptide drugs GLP-1¹⁵⁵ and FGF21¹⁵⁶ have been shown to be effective for 5-10 days in murine models of type 2 diabetes. This approach has also been used to create a bispecific drug where two different protein drugs with complementary pharmacology are fused with an ELP to create a ternary fusion. In the first demonstration of this approach, GLP-1 was fused with FGF-21 via an ELP linker to create a GLP1-ELP-FGF21 fusion. This

bispecific ELP fusion outperformed an equimolar mixture of the GLP1-ELP and ELP-FGF21 fusions, which demonstrated the pharmacological advantages of a unimolecular bispecific drug wherein both drugs are presented from a single molecular scaffold. ELPs have also been used for brachytherapy—intratumoral radiation therapy—wherein a radionuclide is chemically conjugated to a depot-forming ELP, such that, upon injection of the radionuclide—ELP conjugate into a solid tumor, the conjugate phase-separates into an insoluble coacervate that is discretely localized within the tumor and irradiates the tumor from the inside out 157,158 (Figure 5e,f).

Thermally sensitive ELP—drug conjugates can also be engineered to be soluble at body temperature but undergo LLPS-triggered accumulation in tissues that are transiently heated to slightly above body temperature. By externally heating solid tumors to 42 °C, an ELP conjugate with a $T_{\rm t}$ value of $\sim\!40$ °C phase-separates into an aggregate in the tumor, which results in increased tumor localization—even upon the cessation of heating—compared to an ELP control with a $T_{\rm t}$ value of >42 °C, $^{159,160}_{,160}$ and demonstrates that thermal targeting of tumors is possible by mild focused hyperthermia of a solid tumor.

The coacervation of IDPs can also be exploited to trigger selfassembly of nano- and mesoscale structures that carry drugs and present targeting peptides and proteins (Figure 5, inset). This approach requires imparting sufficient amphiphilicity to an ELP to drive its self-assembly into micelles or vesicles. There are three approaches by which this has been achieved. In the first approach, an ELP is fused to a short (CGG)₈ peptide tag, and attachment of hydrophobic molecules with an octanol-water partition coefficient of approximately >1.5 imparts sufficient amphiphilicity to the conjugate to trigger its self-assembly into micelles. 161 Attachment driven assembly of micelles has been used to package a number of hydrophobic small molecule drugs that suffer from poor delivery. For hydrophilic molecules with $\log D$ < 1.5, whose conjugation to the Cys residues does not trigger self-assembly of the ELP into micelles, a hydrophobic $(GGX)_8$ segment (where X = Y, F, or W) is genetically appended to the polypeptide to drive micelle assembly. 162 Adding a drug attachment (CGG)₈ block between the ELP and the selfassembly domain then results in a triblock copolypeptide, and it has been shown that conjugation of hydrophilic small molecule drugs to the Cys residues in the (CGG)₈ domain does not abolish self-assembly into micelles, thereby providing a way to package hydrophilic drugs into nanoparticles. 163 Micelles of these diblock copolypeptides have been used to deliver a range of anticancer chemotherapeutics, such as doxorubicin, paclitaxel, and gemcitabine, in which the conjugated drugs are sequestered in the hydrophobic core of the micelle. In all cases, the nanoparticle formulation of these drugs showed significantly better efficacy than the free drug.

The desolvation of an ELP chain that drives its LCST phase behavior can also be profitably employed to drive temperature-triggered self-assembly. In a diblock ELP (ELP_{BC}) in which one ELP block is significantly more hydrophobic than the second ELP block, with an increase in temperature, the more hydrophobic segment preferentially desolvates and becomes increasingly hydrophobic, and at a critical temperature—the critical micellization temperature (CMT)—the ELP_{BC} self-assembles to form a micelle, with the hydrophobic block in the core, while the solvated, hydrophilic block forms the corona that shields the hydrophobic core. This strategy for ELP self-assembly into micelles was first demonstrated by the Conticello group, ¹⁶⁴ and our group then explored this phenomenon in

greater detail. 165 ELP micelle size can be tuned by varying the block pattern of multiblock ELPs to enable the study of size-dependent nanoparticle tumor accumulation. 166

ELP sequences have been combined with RLPs to form ELP–RLP diblocks. Because RLPs are intrinsically more hydrophobic than ELPs, combining RLP and ELP sequences into block copolymers provides a new approach for self-assembly. Fusing RLP and ELP domains in a diblock sequence results in UCST and LCST behavior within the same molecule and self-assembly into a micelle driven by the architecture of the diblock copolymer. A notable architecture obtained with RLP–ELP conjugates is an elongated cylindrical ("wormlike") micelle. 167

Nanoparticles of A-IDPs can also help solve a universal limitation of most systemically administered nanoparticles that they are preferentially taken up by macrophages that are prevalent in the reticuloendothelial system—mainly in the liver and spleen, causing a high level of accumulation in these organs that can cause significant off-target toxicity. The exterior of these nanoparticles can be engineered to solve this problem by two approaches. The first approach seeks to leverage the fact that albumin has exceptionally long blood circulation and is not taken up to a significant extent in the liver and spleen. To confer these attributes to drug-loaded ELP micelles, an ELP with a (GGC)₈ drug attachment segment on its C-terminus was appended—at the gene level—with a small albumin binding protein domain at the N-terminus. Upon drug attachment, the ELP-drug conjugate self-assembles into micelles, wherein the exterior of the micelles is studded with multiple copies of the albumin-binding protein domain. 168 Upon systemic administration of these drug-loaded ELP nanoparticles, they are immediately coated with an albumin corona, owing to the high—nanomolar—affinity of the albumin binding domain for endogenous serum albumin. These drug-loaded ELP nanoparticles have much longer blood circulation, accumulate in tumors to a much greater extent than undecorated ELP nanoparticles, and show better tumor regression than the control ELP nanoparticles and free drug. A complementary approach simply re-engineers the ELP sequence to incorporate a zwitterionic KE dipeptide in each repeat unit, inspired by the observation that certain zwitterionic polymers have long circulation in blood. 169

These nanoparticles can also be targeted to specific tissues and cell types by decorating the hydrophilic corona of these particles with peptide or protein ligands that bind specific receptors on the surfaces of cells. Surprisingly, worm-like micelles decorated with fibronectin type 3 (FN3) domains had increased avidity for their binding partners, and consequently greater uptake in cells overexpressing integrin receptors compared to unimers, spherical micelles, and even antibodies that targeted the same domains. ¹⁷¹

3.1.4. Macromolecular Materials from Phase-Separating Polymers. While the reversibility of the LLPS of native and artificial IDPs is invaluable for certain applications, such as the purification of biomolecules, there are other applications of IDPs that require solid materials with structural integrity. Polymers with LCST or UCST transitions can be covalently cross-linked as soluble species to form gels, while still retaining their temperature-sensitive ability to exclude solvent. These gels no longer undergo a true phase transition but experience reversible volumetric changes upon reaching their LCST or UCST. PNIPAM, LP, LP, LP, and many other natural and synthetic polymers have been engineered into such gels, which are

useful as tissue engineering scaffolds, ^{176,177} for toxin uptake and drug release, ¹⁷⁵ and the formation of artificial muscles. ¹⁷⁸

Researchers have engineered polypeptides with custom LLPS-driving disordered regions and structure-directing domains to precisely control intermolecular interactions to yield solid materials. Peptides that form coiled-coils were conjugated to PEG and ELP to create network hydrogels with tunable viscoelasticity upon hydration transitions in the gel. 179 Loosely inspired by tropoelastin that has structurally ordered and disordered domains, the inclusion of periodic oligoalanine helices in an ELP scaffold yielded A-IDPs that we termed partially ordered polymers (POPs). POPs exhibit LCST phase behavior similar to ELP but with two important differences. First, POPs have thermal hysteresis in their LCST phase behavior that can be tuned by the fraction of oligoalanine helices in the POP. Second, triggering its phase transition into a coacervate phase does not lead to LLPS; instead, aqueous demixing creates two phases, where the protein-rich phase is a porous solid with a fractal-like structure that is stabilized by intermolecular interactions between the oligoalanine helices in the POP. POPs may prove to be useful as injectable biomaterials for in vivo tissue regeneration, as the porous solid matrix is minimally immunogenic and promotes spontaneous vascularization in mice. 180 Motifs from silk proteins have also been combined with a wide variety of ELPs to control the mechanical stiffness 181 in the hybrid silk-elastin-like proteins.

The phase behavior of A-IDPs and the resultant structures formed upon phase separation can also be modulated—as in native IDPs—by post-translational modification. While posttranslational modification introduces an additional synthetic step following translation, modification can be carried out by coexpressing the enzyme in the same cell as its IDP substrate, effectively making the system entirely genetically encoded. A diblock polypeptide consisting of a C-terminal ELP and a short (5-10 amino acid) N-terminal peptide that both serves as a myristoylation substrate by N-myristoyl transferase (NMT) and as a β -sheet-directing peptide were coexpressed with yeast NMT in E. coli. NMT appended a myristoyl group at the N-terminus of the polypeptide, yielding a fatty-acid-modified ELP (FAME). Depending on their precise sequence, FAMEs can exhibit hierarchical assembly into long tangled fibrils upon the triggering of the LCST transition of ELP, wherein the peptide amphiphile composed of the myristoyl group and β -sheet peptide forms the fibril core, and the ELP forms the hydrophilic corona. The reversibility and hysteresis of these constructs is dependent on the processing temperature, as the FAMEs undergo a reversible transition up to 30 °C but exhibit irreversible or hysteretic assembly above 45 °C depending on their sequence.1

4. CONCLUDING REMARKS

In this Review, we have summarized the underlying physics of aqueous demixing phase behavior, described the experimental methods to characterize and computational methods to simulate this behavior, and followed with illustrative examples of native and artificial IDPs that exhibit LCST and UCST phase behavior and the applications of these proteins in biotechnology and medicine. This field has provided new molecules to engineer phase separation *in vitro* and within cells, such as artificial IDPs—ELPs and RLPs as two prototypical examples—and elegant light triggered systems such as optoDroplets and Corelets. An emerging—and particularly exciting—new effort in this area lies in the engineering of condensates to control

biological function and treat disease, applications that are currently at the proof-of-concept stage and that we foresee will begin to have societal impacts in the next decade.

AUTHOR INFORMATION

Corresponding Author

Ashutosh Chilkoti — Department of Biomedical Engineering, Duke University, Durham, North Carolina 27708, United States; orcid.org/0000-0002-1569-2228; Email: chilkoti@duke.edu

Authors

Daniel Mark Shapiro — Department of Biomedical Engineering, Duke University, Durham, North Carolina 27708, United States; ⊚ orcid.org/0000-0002-8327-2911 Max Ney — Department of Biomedical Engineering, Duke University, Durham, North Carolina 27708, United States Seyed Ali Eghtesadi — Department of Biomedical Engineering, Duke University, Durham, North Carolina 27708, United

Complete contact information is available at: https://pubs.acs.org/10.1021/acs.jpcb.1c01146

Notes

The authors declare no competing financial interest.

Biographies

States



Daniel Mark Shapiro received his B.S. in Physics and Molecular, Cellular, & Developmental Biology from Yale University in 2018, where he worked on engineering electrically conductive protein nanowires produced by bacteria. He's currently a Ph.D. student in the Chilkoti lab at Duke University, where he is working on creating phase-separating protein—RNA condensates using the artificial intrinsically disordered proteins pioneered in the Chilkoti lab. He hopes to work in the biotechnology industry after receiving his doctorate, either as a founder of his own company or working in another start-up.



Max Ney is a Biomedical Engineering Ph.D. student in the Chilkoti Lab at Duke University. His research focuses on the engineering of artificial phase-separating polypeptides with ordered and disordered domains. He began his Ph.D. studies in 2019 after receiving his joint B.S. in Bioengineering and Materials Science and Engineering from the University of California, Berkeley the same year.



Seyed Ali Eghtesadi received his B.S. in Chemistry from Sharif University of Technology. In 2018, he received his Ph.D. in Polymer Science from University of Akron, where he worked on designing stimuli-responsive nanostructures through supramolecular assembly of ionic polymers. He is currently a postdoctoral fellow at the Duke department of Biomedical Engineering, and his research mainly focuses on RNA—protein interactions and engineering ribonucleoprotein granules to provide extrinsic control of protein translation in a cellular environment.



Ashutosh Chilkoti is the Alan L. Kaganov Professor and the Chair of the Department of Biomedical Engineering at Duke University. His areas of research include genetically encoded materials and biointerface science.

He has published ~ 300 papers and is the founder of six start-up companies.

ACKNOWLEDGMENTS

This work was supported in part by the Air Force Office of Scientific Research under AFOSR Award No. FA9550-20-1-0241, the National Institutes of Health grant R35GM127024-3, and the National Science Foundation Designing Materials to Revolutionize and Engineer our Future Grant 1729671.

REFERENCES

- (1) Flory, P. J. Principles of Polymer Chemistry; Cornell University Press: 1953; p 696.
- (2) Huggins, M. L. Solutions of Long Chain Compounds. J. Chem. Phys. 1941, 9 (5), 440.
- (3) Quiroz, F. G.; Chilkoti, A. Sequence heuristics to encode phase behaviour in intrinsically disordered protein polymers. *Nat. Mater.* **2015**, *14* (11), 1164–1171.
- (4) Rubinstein, M.; Colby, R. H. Polymer Physics; OUP Oxford: 2003.
- (5) Brangwynne, C. P.; Tompa, P.; Pappu, R. V. Polymer physics of intracellular phase transitions. *Nat. Phys.* **2015**, *11* (11), 899–904.
- (6) Gandhi, A.; Paul, A.; Sen, S. O.; Sen, K. K. Studies on thermoresponsive polymers: Phase behaviour, drug delivery and biomedical applications. *Asian J. Pharm. Sci.* **2015**, *10* (2), 99–107.
- (7) Miller-Chou, B. A.; Koenig, J. L. A review of polymer dissolution. *Prog. Polym. Sci.* **2003**, 28 (8), 1223–1270.
- (8) Martin, E. W.; Mittag, T. Relationship of Sequence and Phase Separation in Protein Low-Complexity Regions. *Biochemistry* **2018**, *57* (17), 2478–2487.
- (9) Seuring, J.; Agarwal, S. Polymers with Upper Critical Solution Temperature in Aqueous Solution: Unexpected Properties from Known Building Blocks. ACS Macro Lett. 2013, 2 (7), 597–600.
- (10) Sanchez, I. C.; Lacombe, R. H. An elementary molecular theory of classical fluids. J. Phys. Chem. 1976, 80 (21), 2352–2362.
- (11) Alberti, S.; Gladfelter, A.; Mittag, T. Considerations and Challenges in Studying Liquid-Liquid Phase Separation and Biomolecular Condensates. *Cell* **2019**, *176* (3), 419–434.
- (12) Overbeek, J. T. G.; Voorn, M. J. Phase separation in polyelectrolyte solutions. Theory of complex coacervation. *J. Cell. Comp. Physiol.* **1957**, 49 (S1), 7–26.
- (13) Koningsveld, R.; Staverman, A. J. Liquid—liquid phase separation in multicomponent polymer solutions. I. Statement of the problem and description of methods of calculation. *Journal of Polymer Science Part A-2: Polymer Physics* **1968**, 6 (2), 305–323.
- (14) Lin, Y.-H.; Forman-Kay, J. D.; Chan, H. S. Sequence-Specific Polyampholyte Phase Separation in Membraneless Organelles. *Phys. Rev. Lett.* **2016**, *117* (17), 178101.
- (15) Widom, B. Note on the interfacial tension of phase-separated polymer solutions. *J. Stat. Phys.* **1988**, 52 (5), 1343–1351.
- (16) Widom, B. Phase separation in polymer solutions. *Phys. A* **1993**, 194 (1), 532–541.
- (17) Povodyrev, A. A.; Anisimov, M. A.; Sengers, J. V. Crossover Flory model for phase separation in polymer solutions. *Phys. A* **1999**, 264 (3), 345–369.
- (18) Shea, J.-E.; Best, R. B.; Mittal, J. Physics-based computational and theoretical approaches to intrinsically disordered proteins. *Curr. Opin. Struct. Biol.* **2021**, *67*, 219–225.
- (19) Posey, A. E.; Holehouse, A. S.; Pappu, R. V. Phase Separation of Intrinsically Disordered Proteins; Elsevier: 2018; pp 1–30.
- (20) Bischofberger, I.; Trappe, V. New aspects in the phase behaviour of poly-N-isopropyl acrylamide: systematic temperature dependent shrinking of PNiPAM assemblies well beyond the LCST. *Sci. Rep.* **2015**, 5 (1), 15520.
- (21) Roth, P. J.; Jochum, F. D.; Theato, P. UCST-type behavior of poly[oligo(ethylene glycol) methyl ether methacrylate] (POEGMA) in aliphatic alcohols: solvent, co-solvent, molecular weight, and end group dependences. *Soft Matter* **2011**, *7* (6), 2484–2492.

- (22) Dalgakiran, E.; Tatlipinar, H. The role of hydrophobic hydration in the LCST behaviour of POEGMA300 by all-atom molecular dynamics simulations. *Phys. Chem. Chem. Phys.* **2018**, 20 (22), 15389–15399
- (23) Bebis, K.; Jones, M. W.; Haddleton, D. M.; Gibson, M. I. Thermoresponsive behaviour of poly[(oligo(ethyleneglycol methacrylate)]s and their protein conjugates: importance of concentration and solvent system. *Polym. Chem.* **2011**, 2 (4), 975.
- (24) Bae, Y. C.; Lambert, S. M.; Soane, D. S.; Prausnitz, J. M. Cloudpoint curves of polymer solutions from thermooptical measurements. *Macromolecules* **1991**, 24 (15), 4403–4407.
- (25) Saeki, S.; Kuwahara, N.; Nakata, M.; Kaneko, M. Phase separation of poly(ethylene glycol)-water-salt systems. *Polymer* **1977**, *18* (10), 1027–1031.
- (26) Nizardo, N. M.; Schanzenbach, D.; Schönemann, E.; Laschewsky, A. Exploring Poly(ethylene glycol)-Polyzwitterion Diblock Copolymers as Biocompatible Smart Macrosurfactants Featuring UCST-Phase Behavior in Normal Saline Solution. *Polymers* **2018**, *10* (3), 325.
- (27) Seuring, J.; Bayer, F. M.; Huber, K.; Agarwal, S. Upper Critical Solution Temperature of Poly(N-acryloyl glycinamide) in Water: A Concealed Property. *Macromolecules* **2012**, *45* (1), 374–384.
- (28) Cajal, S. R. Un sencillo metodo de coloracion seletiva del reticulo protoplasmatico y sus efectos en los diversos organos nerviosos de vertebrados e invertebrados. *Trab. Lab. Invest. Biol.* (Madrid) 1903, 2, 129–221
- (29) Wagner, R. Einige bemerkungen und fragen über das keimbläschen (vesicular germinativa). Müller's Archiv. Anat. Physiol. Wissenschaft Med. 1835, 268, 373–377.
- (30) Handwerger, K. E.; Cordero, J. A.; Gall, J. G. Cajal Bodies, Nucleoli, and Speckles in the Xenopus Oocyte Nucleus Have a Low-Density, Sponge-like Structure. *Mol. Biol. Cell* **2005**, *16* (1), 202–211.
- (31) Brangwynne, C. P.; Eckmann, C. R.; Courson, D. S.; Rybarska, A.; Hoege, C.; Gharakhani, J.; Jülicher, F.; Hyman, A. A. Germline P Granules Are Liquid Droplets That Localize by Controlled Dissolution/Condensation. *Science* **2009**, 324 (5935), 1729–1732.
- (32) Boeynaems, S.; Alberti, S.; Fawzi, N. L.; Mittag, T.; Polymenidou, M.; Rousseau, F.; Schymkowitz, J.; Shorter, J.; Wolozin, B.; Van Den Bosch, L.; et al. Protein Phase Separation: A New Phase in Cell Biology. *Trends Cell Biol.* **2018**, 28 (6), 420–435.
- (33) Sabari, B. R.; Dall'Agnese, A.; Young, R. A. Biomolecular Condensates in the Nucleus. *Trends Biochem. Sci.* **2020**, *45* (11), 961–977.
- (34) Luo, Y.; Na, Z.; Slavoff, S. A. P-Bodies: Composition, Properties, and Functions. *Biochemistry* **2018**, *57* (17), 2424–2431.
- (35) Mitrea, D. M.; Kriwacki, R. W. Phase separation in biology; functional organization of a higher order. *Cell Commun. Signaling* **2016**, *14* (1), 1.
- (36) Uversky, V. N. Intrinsically disordered proteins in overcrowded milieu: Membrane-less organelles, phase separation, and intrinsic disorder. *Curr. Opin. Struct. Biol.* **2017**, *44*, 18–30.
- (37) Uversky, V. N. Introduction to Intrinsically Disordered Proteins (IDPs). Chem. Rev. 2014, 114 (13), 6557–6560.
- (38) Jakob, U.; Kriwacki, R.; Uversky, V. N. Conditionally and Transiently Disordered Proteins: Awakening Cryptic Disorder To Regulate Protein Function. *Chem. Rev.* **2014**, *114* (13), 6779–6805.
- (39) Vernon, R. M.; Forman-Kay, J. D. First-generation predictors of biological protein phase separation. *Curr. Opin. Struct. Biol.* **2019**, *58*, 88–96.
- (40) Banani, S. F.; Lee, H. O.; Hyman, A. A.; Rosen, M. K. Biomolecular condensates: organizers of cellular biochemistry. *Nat. Rev. Mol. Cell Biol.* **2017**, *18* (5), 285–298.
- (41) van der Lee, R.; Buljan, M.; Lang, B.; Weatheritt, R. J.; Daughdrill, G. W.; Dunker, A. K.; Fuxreiter, M.; Gough, J.; Gsponer, J.; Jones, D. T.; et al. Classification of Intrinsically Disordered Regions and Proteins. *Chem. Rev.* **2014**, *114* (13), 6589–6631.
- (42) Klosin, A.; Oltsch, F.; Harmon, T.; Honigmann, A.; Jülicher, F.; Hyman, A. A.; Zechner, C. Phase separation provides a mechanism to reduce noise in cells. *Science* **2020**, *367* (6476), 464–468.

- (43) Hennig, S.; Kong, G.; Mannen, T.; Sadowska, A.; Kobelke, S.; Blythe, A.; Knott, G. J.; Iyer, K. S.; Ho, D.; Newcombe, E. A.; et al. Prion-like domains in RNA binding proteins are essential for building subnuclear paraspeckles. *J. Cell Biol.* **2015**, *210* (4), 529–539.
- (44) Nott, T. J.; Petsalaki, E.; Farber, P.; Jervis, D.; Fussner, E.; Plochowietz, A.; Craggs, T. D.; Bazett-Jones, D. P.; Pawson, T.; Forman-Kay, J. D.; Baldwin, A. J.; et al. Phase Transition of a Disordered Nuage Protein Generates Environmentally Responsive Membraneless Organelles. *Mol. Cell* **2015**, *57* (5), 936–947.
- (45) Jung, J.-H.; Barbosa, A. D.; Hutin, S.; Kumita, J. R.; Gao, M.; Derwort, D.; Silva, C. S.; Lai, X.; Pierre, E.; Geng, F.; et al. A prion-like domain in ELF3 functions as a thermosensor in Arabidopsis. *Nature* **2020**, 585 (7824), 256–260.
- (46) Stroberg, W.; Schnell, S. Do Cellular Condensates Accelerate Biochemical Reactions? Lessons from Microdroplet Chemistry. *Biophys. J.* **2018**, *115* (1), 3–8.
- (47) Dzuricky, M.; Rogers, B. A.; Shahid, A.; Cremer, P. S.; Chilkoti, A. De novo engineering of intracellular condensates using artificial disordered proteins. *Nat. Chem.* **2020**, *12* (9), 814–825.
- (48) Marnik, E. A.; Updike, D. L. Membraneless organelles: P granules in Caenorhabditis elegans. *Traffic* **2019**, *20* (6), 373–379.
- (49) Burke, K. A.; Janke, A. M.; Rhine, C. L.; Fawzi, N. L. Residue-by-residue view of in vitro FUS granules that bind the C-terminal domain of RNA polymerase II. *Mol. Cell* **2015**, *60* (2), 231–241.
- (50) Patel, A.; Lee, H. O.; Jawerth, L.; Maharana, S.; Jahnel, M.; Hein, M. Y.; Stoynov, S.; Mahamid, J.; Saha, S.; Franzmann, T. M.; Pozniakovski, A.; Poser, I.; Maghelli, N.; Royer, L. A.; Weigert, M.; Myers, E. W.; Grill, S.; Drechsel, D.; Hyman, A. A.; Alberti, S.; et al. A Liquid-to-Solid Phase Transition of the ALS Protein FUS Accelerated by Disease Mutation. *Cell* **2015**, *162* (5), 1066–1077.
- (51) Hernández-Vega, A.; Braun, M.; Scharrel, L.; Jahnel, M.; Wegmann, S.; Hyman, B. T.; Alberti, S.; Diez, S.; Hyman, A. A. Local Nucleation of Microtubule Bundles through Tubulin Concentration into a Condensed Tau Phase. *Cell Rep.* **2017**, 20 (10), 2304–2312.
- (52) Conicella, A. E.; Zerze, G. H.; Mittal, J.; Fawzi, N. L. ALS Mutations Disrupt Phase Separation Mediated by α -Helical Structure in the TDP-43 Low-Complexity C-Terminal Domain. *Structure* **2016**, 24 (9), 1537–1549.
- (53) Mackenzie, I. R.; Nicholson, A. M.; Sarkar, M.; Messing, J.; Purice, M. D.; Pottier, C.; Annu, K.; Baker, M.; Perkerson, R. B.; Kurti, A.; et al. TIA1Mutations in Amyotrophic Lateral Sclerosis and Frontotemporal Dementia Promote Phase Separation and Alter Stress Granule Dynamics. *Neuron* **2017**, *95* (4), 808–816.
- (54) Murthy, A. C.; Dignon, G. L.; Kan, Y.; Zerze, G. H.; Parekh, S. H.; Mittal, J.; Fawzi, N. L. Molecular interactions underlying liquid-liquid phase separation of the FUS low-complexity domain. *Nat. Struct. Mol. Biol.* **2019**, *26* (7), 637–648.
- (55) Malay, A. D.; Suzuki, T.; Katashima, T.; Kono, N.; Arakawa, K.; Numata, K. Spider silk self-assembly via modular liquid-liquid phase separation and nanofibrillation. *Science Advances* **2020**, *6* (45), No. eabb6030.
- (56) Malay, A. D.; Arakawa, K.; Numata, K. Analysis of repetitive amino acid motifs reveals the essential features of spider dragline silk proteins. *PLoS One* **2017**, *12* (8), No. e0183397.
- (57) Iserman, C.; Roden, C. A.; Boerneke, M. A.; Sealfon, R. S. G.; McLaughlin, G. A.; Jungreis, I.; Fritch, E. J.; Hou, Y. J.; Ekena, J.; Weidmann, C. A. Genomic RNA Elements Drive Phase Separation of the SARS-CoV-2 Nucleocapsid. *Mol. Cell* **2020**, *80* (6), 1078–1091.e6.
- (58) Carlson, C. R.; Asfaha, J. B.; Ghent, C. M.; Howard, C. J.; Hartooni, N.; Safari, M.; Frankel, A. D.; Morgan, D. O. Phosphoregulation of Phase Separation by the SARS-CoV-2 N Protein Suggests a Biophysical Basis for its Dual Functions. *Mol. Cell* **2020**, *80*, 1092–1103.e4.
- (59) Somjee, R.; Mitrea, D. M.; Kriwacki, R. W. Exploring Relationships between the Density of Charged Tracts within Disordered Regions and Phase Separation. *In Biocomputing* **2020**, 207–218.
- (60) Pak, C. W.; Kosno, M.; Holehouse, A. S.; Padrick, S. B.; Mittal, A.; Ali, R.; Yunus, A. A.; Liu, D. R.; Pappu, R. V.; Rosen, M. K. Sequence

- Determinants of Intracellular Phase Separation by Complex Coacervation of a Disordered Protein. *Mol. Cell* **2016**, *63* (1), 72–85.
- (61) Bianchi, G.; Longhi, S.; Grandori, R.; Brocca, S. Relevance of Electrostatic Charges in Compactness, Aggregation, and Phase Separation of Intrinsically Disordered Proteins. *Int. J. Mol. Sci.* **2020**, 21 (17), 6208.
- (62) Garcia-Jove Navarro, M.; Kashida, S.; Chouaib, R.; Souquere, S.; Pierron, G.; Weil, D.; Gueroui, Z. RNA is a critical element for the sizing and the composition of phase-separated RNA-protein condensates. *Nat. Commun.* **2019**, *10* (1), 3230.
- (63) Banerjee, P. R.; Milin, A. N.; Moosa, M. M.; Onuchic, P. L.; Deniz, A. A. Reentrant Phase Transition Drives Dynamic Substructure Formation in Ribonucleoprotein Droplets. *Angew. Chem., Int. Ed.* **2017**, 56 (38), 11354–11359.
- (64) Alshareedah, I.; Kaur, T.; Ngo, J.; Seppala, H.; Kounatse, L.-A. D.; Wang, W.; Moosa, M. M.; Banerjee, P. R. Interplay between Short-Range Attraction and Long-Range Repulsion Controls Reentrant Liquid Condensation of Ribonucleoprotein-RNA Complexes. *J. Am. Chem. Soc.* 2019, 141 (37), 14593–14602.
- (65) King, O. D.; Gitler, A. D.; Shorter, J. The tip of the iceberg: RNA-binding proteins with prion-like domains in neurodegenerative disease. *Brain Res.* **2012**, *1462*, 61–80.
- (66) Schmidt, H. B.; Barreau, A.; Rohatgi, R. Phase separation-deficient TDP43 remains functional in splicing. *Nat. Commun.* **2019**, *10* (1), 4890.
- (67) Maharana, S.; Wang, J.; Papadopoulos, D. K.; Richter, D.; Pozniakovsky, A.; Poser, I.; Bickle, M.; Rizk, S.; Guillén-Boixet, J.; Franzmann, T. M.; et al. RNA buffers the phase separation behavior of prion-like RNA binding proteins. *Science* **2018**, *360* (6391), 918–921.
- (68) Roden, C.; Gladfelter, A. S. RNA contributions to the form and function of biomolecular condensates. *Nat. Rev. Mol. Cell Biol.* **2021**, 22 (3), 183–195.
- (69) St George-Hyslop, P.; Lin, J. Q.; Miyashita, A.; Phillips, E. C.; Qamar, S.; Randle, S. J.; Wang, G. The physiological and pathological biophysics of phase separation and gelation of RNA binding proteins in amyotrophic lateral sclerosis and fronto-temporal lobar degeneration. *Brain Res.* **2018**, *1693*, 11–23.
- (70) Li, P.; Banjade, S.; Cheng, H.-C.; Kim, S.; Chen, B.; Guo, L.; Llaguno, M.; Hollingsworth, J. V.; King, D. S.; Banani, S. F.; et al. Phase transitions in the assembly of multivalent signalling proteins. *Nature* **2012**, *483* (7389), 336–340.
- (71) Banani, S. F.; Rice, A. M.; Peeples, W. B.; Lin, Y.; Jain, S.; Parker, R.; Rosen, M. K. Compositional Control of Phase-Separated Cellular Bodies. *Cell* **2016**, *166* (3), *651–663*.
- (72) Franzmann, T. M.; Jahnel, M.; Pozniakovsky, A.; Mahamid, J.; Holehouse, A. S.; Nüske, E.; Richter, D.; Baumeister, W.; Grill, S. W.; Pappu, R. V.; et al. Phase separation of a yeast prion protein promotes cellular fitness. *Science* **2018**, 359 (6371), No. eaao5654.
- (73) Ruff, K. M.; Roberts, S.; Chilkoti, A.; Pappu, R. V. Advances in Understanding Stimulus-Responsive Phase Behavior of Intrinsically Disordered Protein Polymers. J. Mol. Biol. 2018, 430 (23), 4619–4635.
- (74) Carisey, A.; Stroud, M.; Tsang, R.; Ballestrem, C. Fluorescence Recovery After Photobleaching. In *Cell Migration: Developmental Methods and Protocols*; Wells, C. M., Parsons, M., Eds.; Humana Press: Totowa, NJ, 2011; pp 387–402.
- (75) Babinchak, W. M.; Haider, R.; Dumm, B. K.; Sarkar, P.; Surewicz, K.; Choi, J.-K.; Surewicz, W. K. The role of liquid-liquid phase separation in aggregation of the TDP-43 low-complexity domain. *J. Biol. Chem.* **2019**, *294* (16), 6306–6317.
- (76) Wang, Z.; Zhang, G.; Zhang, H. Protocol for analyzing protein liquid-liquid phase separation. *Biophysics Reports* **2019**, 5 (1), 1–9.
- (77) Monahan, Z.; Ryan, V. H.; Janke, A. M.; Burke, K. A.; Rhoads, S. N.; Zerze, G. H.; O'Meally, R.; Dignon, G. L.; Conicella, A. E.; Zheng, W.; et al. Phosphorylation of the FUS low-complexity domain disrupts phase separation, aggregation, and toxicity. *EMBO J.* **2017**, *36* (20), 2951–2967.
- (78) Jensen, M. R.; Zweckstetter, M.; Huang, J.-r.; Blackledge, M. Exploring Free-Energy Landscapes of Intrinsically Disordered Proteins

- at Atomic Resolution Using NMR Spectroscopy. *Chem. Rev.* **2014**, *114* (13), 6632–6660.
- (79) Bhattarai, A.; Emerson, I. A. Dynamic conformational flexibility and molecular interactions of intrinsically disordered proteins. *J. Biosci.* **2020**, 45 (1), 29.
- (80) Solomon, I. Relaxation Processes in a System of Two Spins. *Phys. Rev.* **1955**, 99 (2), 559–565.
- (81) Kosol, S.; Contreras-Martos, S.; Cedeño, C.; Tompa, P. Structural Characterization of Intrinsically Disordered Proteins by NMR Spectroscopy. *Molecules* **2013**, *18* (9), 10802.
- (82) Wells, M.; Tidow, H.; Rutherford, T. J.; Markwick, P.; Jensen, M. R.; Mylonas, E.; Svergun, D. I.; Blackledge, M.; Fersht, A. R. Structure of tumor suppressor p53 and its intrinsically disordered N-terminal transactivation domain. *Proc. Natl. Acad. Sci. U. S. A.* **2008**, *105* (15), 5762.
- (83) Allison, J. R.; Varnai, P.; Dobson, C. M.; Vendruscolo, M. Determination of the Free Energy Landscape of α -Synuclein Using Spin Label Nuclear Magnetic Resonance Measurements. *J. Am. Chem. Soc.* **2009**, *131* (51), 18314–18326.
- (84) Mukrasch, M. D.; Bibow, S.; Korukottu, J.; Jeganathan, S.; Biernat, J.; Griesinger, C.; Mandelkow, E.; Zweckstetter, M. Structural Polymorphism of 441-Residue Tau at Single Residue Resolution. *PLoS Biol.* **2009**, *7* (2), No. e1000034.
- (85) Ryan, V. H.; Dignon, G. L.; Zerze, G. H.; Chabata, C. V.; Silva, R.; Conicella, A. E.; Amaya, J.; Burke, K. A.; Mittal, J.; Fawzi, N. L. Mechanistic View of hnRNPA2 Low-Complexity Domain Structure, Interactions, and Phase Separation Altered by Mutation and Arginine Methylation. *Mol. Cell* **2018**, *69* (3), 465–479.
- (86) Bernadó, P.; Mylonas, E.; Petoukhov, M. V.; Blackledge, M.; Svergun, D. I. Structural Characterization of Flexible Proteins Using Small-Angle X-ray Scattering. *J. Am. Chem. Soc.* **2007**, *129* (17), 5656–5664.
- (87) Svergun, D. Determination of the regularization parameter in indirect-transform methods using perceptual criteria. *J. Appl. Crystallogr.* **1992**, 25 (4), 495–503.
- (88) Gabel, F., Small Angle Neutron Scattering for the Structural Study of Intrinsically Disordered Proteins in Solution: A Practical Guide. In *Intrinsically Disordered Protein Analysis: Vol. 2, Methods and Experimental Tools*; Uversky, V. N., Dunker, A. K., Eds.; Springer: New York, 2012; pp 123–135.
- (89) Graewert, M. A.; Svergun, D. I. Impact and progress in small and wide angle X-ray scattering (SAXS and WAXS). *Curr. Opin. Struct. Biol.* **2013**, 23 (5), 748–754.
- (90) Ferreon, A. C. M.; Moran, C. R.; Gambin, Y.; Deniz, A. A. Chapter 10 Single-Molecule Fluorescence Studies of Intrinsically Disordered Proteins. In *Methods in Enzymology*; Walter, N. G., Ed.; Academic Press: 2010; Vol. 472, pp 179–204.
- (91) Jawerth, L. M.; Ijavi, M.; Ruer, M.; Saha, S.; Jahnel, M.; Hyman, A. A.; Jülicher, F.; Fischer-Friedrich, E. Salt-Dependent Rheology and Surface Tension of Protein Condensates Using Optical Traps. *Phys. Rev. Lett.* **2018**, *121* (25), 258101.
- (92) Permyakov, S. E. Differential Scanning Microcalorimetry of Intrinsically Disordered Proteins; Springer: New York, 2012; pp 283–296
- (93) Johnson, C. M. Differential scanning calorimetry as a tool for protein folding and stability. *Arch. Biochem. Biophys.* **2013**, *531* (1–2), 100–109.
- (94) Ibarra-Molero, B.; Naganathan, A. N.; Sanchez-Ruiz, J. M.; Muñoz, V. Modern Analysis of Protein Folding by Differential Scanning Calorimetry; Elsevier: 2016; pp 281–318.
- (95) Giri Rao, V. H.; Gosavi, S. Using the folding landscapes of proteins to understand protein function. *Curr. Opin. Struct. Biol.* **2016**, 36, 67–74.
- (96) Mazurenko, S.; Kunka, A.; Beerens, K.; Johnson, C. M.; Damborsky, J.; Prokop, Z. Exploration of Protein Unfolding by Modelling Calorimetry Data from Reheating. *Sci. Rep.* **2017**, *7* (1), 16321.

- (97) Dzwolak, W.; Ravindra, R.; Lendermann, J.; Winter, R. Aggregation of Bovine Insulin Probed by DSC/PPC Calorimetry and FTIR Spectroscopy. *Biochemistry* **2003**, 42 (38), 11347–11355.
- (98) Tompa, P.; Han, K.-H.; Bokor, M.; Kamasa, P.; Tantos, A.; Fritz, B.; Kim, D.-H.; Lee, C.; Verebelyi, T.; Tompa, K. Wide-line NMR and DSC studies on intrinsically disordered p53 transactivation domain and its helically pre-structured segment. *BMB Reports* **2016**, 49 (9), 497–501.
- (99) Halpern, H. J.; Spencer, D. P.; Van Polen, J.; Bowman, M. K.; Nelson, A. C.; Dowey, E. M.; Teicher, B. A. Imaging radio frequency electron-spin-resonance spectrometer with high resolution and sensitivity forinvivomeasurements. *Rev. Sci. Instrum.* **1989**, *60* (6), 1040–1050
- (100) Le Breton, N.; Martinho, M. N.; Mileo, E.; Etienne, E.; Gerbaud, G.; Guigliarelli, B.; Belle, V. R. Exploring intrinsically disordered proteins using site-directed spin labeling electron paramagnetic resonance spectroscopy. *Frontiers in Molecular Biosciences* **2015**, DOI: 10.3389/fmolb.2015.00021.
- (101) Drescher, M. EPR in Protein Science; Springer: Berlin, Heidelberg, 2011; pp 91-119.
- (102) Haustein, E. Ultrasensitive investigations of biological systems by fluorescence correlation spectroscopy. *Methods* **2003**, 29 (2), 153–166.
- (103) Sahoo, B.; Drombosky, K. W.; Wetzel, R. Fluorescence Correlation Spectroscopy: A Tool to Study Protein Oligomerization and Aggregation In Vitro and In Vivo; Springer: New York, 2016; pp 67–87.
- (104) Alshareedah, I.; Thurston, G. M.; Banerjee, P. R. Quantifying viscosity and surface tension of multicomponent protein-nucleic acid condensates. *Biophys. J.* 2021, 120, 1161.
- (105) Peng, S.; Li, W.; Yao, Y.; Xing, W.; Li, P.; Chen, C. Phase separation at the nanoscale quantified by dcFCCS. *Proc. Natl. Acad. Sci. U. S. A.* **2020**, *117* (44), 27124–27131.
- (106) Wei, M.-T.; Elbaum-Garfinkle, S.; Holehouse, A. S.; Chen, C. C.-H.; Feric, M.; Arnold, C. B.; Priestley, R. D.; Pappu, R. V.; Brangwynne, C. P. Phase behaviour of disordered proteins underlying low density and high permeability of liquid organelles. *Nat. Chem.* **2017**, 9 (11), 1118–1125.
- (107) Das, P.; Matysiak, S.; Mittal, J. Looking at the Disordered Proteins through the Computational Microscope. ACS Cent. Sci. 2018, 4 (5), 534–542.
- (108) Ren, S. R.; Hamley, I. W. Cell Dynamics Simulations of Microphase Separation in Block Copolymers. *Macromolecules* **2001**, 34 (1), 116–126.
- (109) Berry, J.; Brangwynne, C. P.; Haataja, M. Physical principles of intracellular organization via active and passive phase transitions. *Rep. Prog. Phys.* **2018**, *81* (4), 046601.
- (110) Falahati, H.; Haji-Akbari, A. Thermodynamically driven assemblies and liquid-liquid phase separations in biology. *Soft Matter* **2019**, *15* (6), 1135–1154.
- (111) Fredrickson, G. H.; Ganesan, V.; Drolet, F. Field-Theoretic Computer Simulation Methods for Polymers and Complex Fluids. *Macromolecules* **2002**, *35* (1), 16–39.
- (112) Fredrickson, G. The equilibrium theory of inhomogeneous polymers; Oxford University Press on Demand: 2006; Vol. 134.
- (113) Wolde, P. R. t.; Frenkel, D. Enhancement of Protein Crystal Nucleation by Critical Density Fluctuations. *Science* **1997**, 277 (5334), 1975–1978.
- (114) Doye, J. P. K.; Louis, A. A.; Lin, I. C.; Allen, L. R.; Noya, E. G.; Wilber, A. W.; Kok, H. C.; Lyus, R. Controlling crystallization and its absence: proteins, colloids and patchy models. *Phys. Chem. Chem. Phys.* **2007**, *9* (18), 2197–2205.
- (115) Gögelein, C.; Nägele, G.; Tuinier, R.; Gibaud, T.; Stradner, A.; Schurtenberger, P. A simple patchy colloid model for the phase behavior of lysozyme dispersions. *J. Chem. Phys.* **2008**, *129* (8), 085102.
- (116) Kim, B.; Chilkoti, A. Allosteric Actuation of Inverse Phase Transition of a Stimulus-Responsive Fusion Polypeptide by Ligand Binding. *J. Am. Chem. Soc.* **2008**, *130* (52), 17867–17873.
- (117) Paloni, M.; Bailly, R.; Ciandrini, L.; Barducci, A. Unraveling Molecular Interactions in Liquid-Liquid Phase Separation of

- Disordered Proteins by Atomistic Simulations. J. Phys. Chem. B 2020, 124 (41), 9009–9016.
- (118) Das, S.; Eisen, A.; Lin, Y.-H.; Chan, H. S. A Lattice Model of Charge-Pattern-Dependent Polyampholyte Phase Separation. *J. Phys. Chem. B* **2018**, 122 (21), 5418–5431.
- (119) Alder, B. J.; Wainwright, T. E. Studies in Molecular Dynamics. I. General Method. *J. Chem. Phys.* **1959**, *31* (2), 459–466.
- (120) Robustelli, P.; Piana, S.; Shaw, D. E. Developing a molecular dynamics force field for both folded and disordered protein states. *Proc. Natl. Acad. Sci. U. S. A.* **2018**, *115* (21), E4758–E4766.
- (121) Lindorff-Larsen, K.; Maragakis, P.; Piana, S.; Eastwood, M. P.; Dror, R. O.; Shaw, D. E. Systematic Validation of Protein Force Fields against Experimental Data. *PLoS One* **2012**, *7* (2), No. e32131.
- (122) Panagiotopoulos, A. Z.; Quirke, N.; Stapleton, M.; Tildesley, D. J. Phase equilibria by simulation in the Gibbs ensemble. *Mol. Phys.* **1988**, *63* (4), 527–545.
- (123) Urry, D. W.; Gowda, D. C.; Parker, T. M.; Luan, C.-H.; Reid, M. C.; Harris, C. M.; Pattanaik, A.; Harris, R. D. Hydrophobicity scale for proteins based on inverse temperature transitions. *Biopolymers* **1992**, 32 (9), 1243–1250.
- (124) Nuhn, H.; Klok, H.-A. Secondary Structure Formation and LCST Behavior of Short Elastin-Like Peptides. *Biomacromolecules* **2008**, *9* (10), 2755–2763.
- (125) Roberts, S.; Dzuricky, M.; Chilkoti, A. Elastin-like Polypeptides as Models of Intrinsically Disordered Proteins. *FEBS Lett.* **2015**, *589*, 2477–2486.
- (126) Amiram, M.; Quiroz, F. G.; Callahan, D. J.; Chilkoti, A. A highly parallel method for synthesizing DNA repeats enables the discovery of 'smart' protein polymers. *Nat. Mater.* **2011**, *10* (2), 141–148.
- (127) Garcia Quiroz, F.; Li, N. K.; Roberts, S.; Weber, P.; Dzuricky, M.; Weitzhandler, I.; Yingling, Y. G.; Chilkoti, A. Intrinsically disordered proteins access a range of hysteretic phase separation behaviors. *Science Advances* **2019**, *5* (10), No. eaax5177.
- (128) Balu, R.; Dutta, N. K.; Choudhury, N. R.; Elvin, C. M.; Lyons, R. E.; Knott, R.; Hill, A. J. An16-resilin: An advanced multi-stimuli-responsive resilin-mimetic protein polymer. *Acta Biomater.* **2014**, *10* (11), 4768–4777.
- (129) Shin, Y.; Brangwynne, C. P. Liquid phase condensation in cell physiology and disease. *Science* **2017**, *357* (6357), No. eaaf4382.
- (130) Wang, J.; Choi, J.-M.; Holehouse, A. S.; Lee, H. O.; Zhang, X.; Jahnel, M.; Maharana, S.; Lemaitre, R.; Pozniakovsky, A.; Drechsel, D.; et al. A Molecular Grammar Governing the Driving Forces for Phase Separation of Prion-like RNA Binding Proteins. *Cell* **2018**, *174* (3), 688–699.
- (131) Shin, Y.; Berry, J.; Pannucci, N.; Haataja, M. P.; Toettcher, J. E.; Brangwynne, C. P. Spatiotemporal control of intracellular phase transitions using light-activated optoDroplets. *Cell* **2017**, *168* (1–2), 159–171.
- (132) Bracha, D.; Walls, M. T.; Wei, M.-T.; Zhu, L.; Kurian, M.; Avalos, J. L.; Toettcher, J. E.; Brangwynne, C. P. Mapping local and global liquid phase behavior in living cells using photo-oligomerizable seeds. *Cell* **2018**, *175* (6), 1467–1480.
- (133) Bracha, D.; Walls, M. T.; Brangwynne, C. P. Probing and engineering liquid-phase organelles. *Nat. Biotechnol.* **2019**, *37*, 1435–1445.
- (134) Dine, E.; Gil, A. A.; Uribe, G.; Brangwynne, C. P.; Toettcher, J. E. Protein phase separation provides long-term memory of transient spatial stimuli. *Cell systems* **2018**, *6* (6), 655–663.
- (135) Shin, Y.; Chang, Y.-C.; Lee, D. S.; Berry, J.; Sanders, D. W.; Ronceray, P.; Wingreen, N. S.; Haataja, M.; Brangwynne, C. P. Liquid nuclear condensates mechanically sense and restructure the genome. *Cell* **2018**, 175 (6), 1481–1491.
- (136) Li, Z.; Tyrpak, D. R.; Park, M.; Okamoto, C. T.; MacKay, J. A. A new temperature-dependent strategy to modulate the epidermal growth factor receptor. *Biomaterials* **2018**, *183*, 319—330.
- (137) Simon, J. R.; Eghtesadi, S. A.; Dzuricky, M.; You, L.; Chilkoti, A. Engineered Ribonucleoprotein Granules Inhibit Translation in Protocells. *Mol. Cell* **2019**, *75* (1), *66*–*75*.

- (138) Reinkemeier, C. D.; Girona, G. E.; Lemke, E. A. Designer membraneless organelles enable codon reassignment of selected mRNAs in eukaryotes. *Science* **2019**, *363* (6434), No. eaaw2644.
- (139) Hassouneh, W.; Christensen, T.; Chilkoti, A. Elastin-like polypeptides as a purification tag for recombinant proteins. *Current protocols in protein science* **2010**, *61* (1), *6.11.1–6.11.16*.
- (140) Meyer, D. E.; Trabbic-Carlson, K.; Chilkoti, A. Protein Purification by Fusion with an Environmentally Responsive Elastin-Like Polypeptide: Effect of Polypeptide Length on the Purification of Thioredoxin. *Biotechnol. Prog.* **2001**, *17* (4), 720–728.
- (141) Bellucci, J. J.; Amiram, M.; Bhattacharyya, J.; McCafferty, D.; Chilkoti, A. Three-in-one chromatography-free purification, tag removal, and site-specific modification of recombinant fusion proteins using sortase A and elastin-like polypeptides. *Angew. Chem., Int. Ed.* **2013**, 52 (13), 3703–3708.
- (142) Shi, C.; Meng, Q.; Wood, D. W. A dual ELP-tagged split intein system for non-chromatographic recombinant protein purification. *Appl. Microbiol. Biotechnol.* **2013**, 97 (2), 829–835.
- (143) Lyons, R. E.; Elvin, C. M.; Taylor, K.; Lekieffre, N.; Ramshaw, J. A. Purification of recombinant protein by cold-coacervation of fusion constructs incorporating resilin-inspired polypeptides. *Biotechnol. Bioeng.* **2012**, *109* (12), 2947–2954.
- (144) Xu, Y.; Mazzawi, M.; Chen, K.; Sun, L.; Dubin, P. L. Protein purification by polyelectrolyte coacervation: influence of protein charge anisotropy on selectivity. *Biomacromolecules* **2011**, *12* (5), 1512–1522.
- (145) Kim, J. Y.; Mulchandani, A.; Chen, W. Temperature-triggered purification of antibodies. *Biotechnol. Bioeng.* **2005**, *90* (3), 373–379.
- (146) Madan, B.; Chaudhary, G.; Cramer, S. M.; Chen, W. ELP-z and ELP-zz capturing scaffolds for the purification of immunoglobulins by affinity precipitation. *J. Biotechnol.* **2013**, *163* (1), 10–16.
- (147) Kostal, J.; Mulchandani, A.; Chen, W. Affinity purification of plasmid DNA by temperature-triggered precipitation. *Biotechnol. Bioeng.* **2004**, *85* (3), 293–297.
- (148) Kim, H.; Chen, W. A non-chromatographic protein purification strategy using Src 3 homology domains as generalized capture domains. *J. Biotechnol.* **2016**, 234, 27–34.
- (149) Mullerpatan, A.; Chandra, D.; Kane, E.; Karande, P.; Cramer, S. Purification of proteins using peptide-ELP based affinity precipitation. *J. Biotechnol.* **2020**, 309, 59–67.
- (150) Ozer, I.; Chilkoti, A. Site-specific and stoichiometric stealth polymer conjugates of therapeutic peptides and proteins. *Bioconjugate Chem.* **2017**, 28 (3), 713–723.
- (151) MacEwan, S. R.; Chilkoti, A. Elastin-like polypeptides: biomedical applications of tunable biopolymers. *Biopolymers* **2010**, *94* (1), 60–77.
- (152) Trabbic-Carlson, K.; Meyer, D.; Liu, L.; Piervincenzi, R.; Nath, N.; LaBean, T.; Chilkoti, A. Effect of protein fusion on the transition temperature of an environmentally responsive elastin-like polypeptide: a role for surface hydrophobicity? *Protein Eng., Des. Sel.* **2004**, *17* (1), 57–66.
- (153) Shamji, M. F.; Betre, H.; Kraus, V. B.; Chen, J.; Chilkoti, A.; Pichika, R.; Masuda, K.; Setton, L. A. Development and characterization of a fusion protein between thermally responsive elastin-like polypeptide and interleukin-1 receptor antagonist: Sustained release of a local antiinflammatory therapeutic. *Arthritis Rheum.* **2007**, *56* (11), 3650–3661.
- (154) Liu, W.; MacKay, J. A.; Dreher, M. R.; Chen, M.; McDaniel, J. R.; Simnick, A. J.; Callahan, D. J.; Zalutsky, M. R.; Chilkoti, A. Injectable intratumoral depot of thermally responsive polypeptide-radionuclide conjugates delays tumor progression in a mouse model. *J. Controlled Release* **2010**, 144 (1), 2–9.
- (155) Amiram, M.; Luginbuhl, K.; Li, X.; Feinglos, M.; Chilkoti, A. A depot-forming glucagon-like peptide-1 fusion protein reduces blood glucose for five days with a single injection. *J. Controlled Release* **2013**, 172 (1), 144–151.
- (156) Gilroy, C. A.; Roberts, S.; Chilkoti, A. Fusion of fibroblast growth factor 21 to a thermally responsive biopolymer forms an injectable depot with sustained anti-diabetic action. *J. Controlled Release* **2018**, 277, 154–164.

- (157) Liu, W.; McDaniel, J.; Li, X.; Asai, D.; Quiroz, F. G.; Schaal, J.; Park, J. S.; Zalutsky, M.; Chilkoti, A. Brachytherapy Using Injectable Seeds That Are Self-Assembled from Genetically Encoded Polypeptides *In Situ. Cancer Res.* **2012**, *72* (22), 5956.
- (158) Mukerji, R.; Schaal, J.; Li, X.; Bhattacharyya, J.; Asai, D.; Zalutsky, M. R.; Chilkoti, A.; Liu, W. Spatiotemporally photoradiation-controlled intratumoral depot for combination of brachytherapy and photodynamic therapy for solid tumor. *Biomaterials* **2016**, *79*, 79–87.
- (159) Meyer, D. E.; Kong, G. A.; Dewhirst, M. W.; Zalutsky, M. R.; Chilkoti, A. Targeting a genetically engineered elastin-like polypeptide to solid tumors by local hyperthermia. *Cancer Res.* **2001**, *61* (4), 1548–1554.
- (160) Dreher, M. R.; Liu, W.; Michelich, C. R.; Dewhirst, M. W.; Chilkoti, A. Thermal cycling enhances the accumulation of a temperature-sensitive biopolymer in solid tumors. *Cancer Res.* **2007**, 67 (9), 4418–4424.
- (161) McDaniel, J. R.; Bhattacharyya, J.; Vargo, K. B.; Hassouneh, W.; Hammer, D. A.; Chilkoti, A. Self-assembly of thermally responsive nanoparticles of a genetically encoded peptide polymer by drug conjugation. *Angew. Chem., Int. Ed.* **2013**, *52* (6), 1683–1687.
- (162) McDaniel, J. R.; Weitzhandler, I.; Prevost, S.; Vargo, K. B.; Appavou, M.-S.; Hammer, D. A.; Gradzielski, M.; Chilkoti, A. Noncanonical Self-Assembly of Highly Asymmetric Genetically Encoded Polypeptide Amphiphiles into Cylindrical Micelles. *Nano Lett.* **2014**, *14* (11), 6590–6598.
- (163) Bhattacharyya, J.; Weitzhandler, I.; Ho, S. B.; McDaniel, J. R.; Li, X.; Tang, L.; Liu, J.; Dewhirst, M.; Chilkoti, A. Encapsulating a Hydrophilic Chemotherapeutic into Rod-Like Nanoparticles of a Genetically Encoded Asymmetric Triblock Polypeptide Improves Its Efficacy. *Adv. Funct. Mater.* **2017**, 27 (12), 1605421.
- (164) Lee, T. A. T.; Cooper, A.; Apkarian, R. P.; Conticello, V. P. Thermo-Reversible Self-Assembly of Nanoparticles Derived from Elastin-Mimetic Polypeptides. *Adv. Mater.* **2000**, *12* (15), 1105–1110.
- (165) Dreher, M. R.; Simnick, A. J.; Fischer, K.; Smith, R. J.; Patel, A.; Schmidt, M.; Chilkoti, A. Temperature Triggered Self-Assembly of Polypeptides into Multivalent Spherical Micelles. *J. Am. Chem. Soc.* **2008**, 130 (2), 687–694.
- (166) MacEwan, S. R.; Weitzhandler, I.; Hoffmann, I.; Genzer, J.; Gradzielski, M.; Chilkoti, A. Phase behavior and self-assembly of perfectly sequence-defined and monodisperse multiblock copolypeptides. *Biomacromolecules* **2017**, *18* (2), 599–609.
- (167) Weitzhandler, I.; Dzuricky, M.; Hoffmann, I.; Garcia Quiroz, F.; Gradzielski, M.; Chilkoti, A. Micellar Self-Assembly of Recombinant Resilin-/Elastin-Like Block Copolypeptides. *Biomacromolecules* **2017**, 18 (8), 2419–2426.
- (168) Yousefpour, P.; McDaniel, J. R.; Prasad, V.; Ahn, L.; Li, X.; Subrahmanyan, R.; Weitzhandler, I.; Suter, S.; Chilkoti, A. Genetically Encoding Albumin Binding into Chemotherapeutic-loaded Polypeptide Nanoparticles Enhances Their Antitumor Efficacy. *Nano Lett.* **2018**, *18* (12), 7784–7793.
- (169) Banskota, S.; Yousefpour, P.; Kirmani, N.; Li, X.; Chilkoti, A. Long circulating genetically encoded intrinsically disordered zwitterionic polypeptides for drug delivery. *Biomaterials* **2019**, *192*, 475–485.
- (170) Wang, J.; Min, J.; Eghtesadi, S. A.; Kane, R. S.; Chilkoti, A. Quantitative Study of the Interaction of Multivalent Ligand-Modified Nanoparticles with Breast Cancer Cells with Tunable Receptor Density. ACS Nano 2020, 14 (1), 372–383.
- (171) Dzuricky, M.; Xiong, S.; Weber, P.; Chilkoti, A. Avidity and Cell Uptake of Integrin-Targeting Polypeptide Micelles is Strongly Shape-Dependent. *Nano Lett.* **2019**, *19* (9), 6124–6132.
- (172) Tanaka, T. Phase transitions in gels and a single polymer. Polymer 1979, 20 (11), 1404-1412.
- (173) Yoshida, R.; Sakai, K.; Okano, T.; Sakurai, Y. Modulating the phase transition temperature and thermosensitivity in N-isopropylacrylamide copolymer gels. *J. Biomater. Sci., Polym. Ed.* **1995**, *6* (6), 585–598.
- (174) Trabbic-Carlson, K.; Setton, L. A.; Chilkoti, A. Swelling and Mechanical Behaviors of Chemically Cross-Linked Hydrogels of Elastin-like Polypeptides. *Biomacromolecules* **2003**, *4* (3), 572–580.

- (175) Amiya, T.; Tanaka, T. Phase transitions in crosslinked gels of natural polymers. Macromolecules 1987, 20 (5), 1162-1164.
- (176) Rodríguez Cabello, J. C.; De Torre, I. G.; Cipriani, F.; Poocza, L. Elastin-like materials for tissue regeneration and repair. In Peptides and Proteins as Biomaterials for Tissue Regeneration and Repair; Barbosa, M. A., Martins, M. C. L., Eds.; Woodhead Publishing: 2018; pp 309-327. (177) Lim, D. W.; Nettles, D. L.; Setton, L. A.; Chilkoti, A. In Situ

Cross-Linking of Elastin-like Polypeptide Block Copolymers for Tissue Repair. Biomacromolecules 2008, 9 (1), 222-230.

- (178) Hidaka, M.; Yoshida, R. Self-oscillating gel composed of thermosensitive polymer exhibiting higher LCST. J. Controlled Release **2011**, 150 (2), 171–176.
- (179) Dooling, L. J.; Buck, M. E.; Zhang, W.-B.; Tirrell, D. A. Programming Molecular Association and Viscoelastic Behavior in Protein Networks. Adv. Mater. 2016, 28 (23), 4651-4657.
- (180) Roberts, S.; Harmon, T. S.; Schaal, J. L.; Miao, V.; Li, K.; Hunt, A.; Wen, Y.; Oas, T. G.; Collier, J. H.; Pappu, R. V.; et al. Injectable tissue integrating networks from recombinant polypeptides with tunable order. Nat. Mater. 2018, 17 (12), 1154-1163.
- (181) Xia, X.-X.; Xu, Q.; Hu, X.; Qin, G.; Kaplan, D. L. Tunable Self-Assembly of Genetically Engineered Silk-Elastin-like Protein Polymers. Biomacromolecules 2011, 12 (11), 3844-3850.
- (182) Mozhdehi, D.; Luginbuhl, K. M.; Simon, J. R.; Dzuricky, M.; Berger, R.; Varol, H. S.; Huang, F. C.; Buehne, K. L.; Mayne, N. R.; Weitzhandler, I.; et al. Genetically encoded lipid-polypeptide hybrid biomaterials that exhibit temperature-triggered hierarchical selfassembly. Nat. Chem. 2018, 10 (5), 496-505.